

Comparison of different methods for the determination of sunshine duration

Yvonne B.L. Hinssen

Scientific report = wetenschappelijk rapport; WR 2006-06

De Bilt, 2006

PO Box 201
3730 AE De Bilt
Wilhelminalaan 10
De Bilt
The Netherlands
<http://www.knmi.nl>
Telephone +31(0)30-220 69 11
Telefax +31(0)30-221 04 07

Author: Hinssen, Y.B.L.
(University of Utrecht)



Scientific report; WR-2006-xx

Comparison of different methods for the determination of sunshine duration

Yvonne B.L. Hinssen

Contents

1. Introduction	5
2. Instruments for the measurement of solar radiation	9
2.1. Pyrheliometer	9
2.2. Pyranometer	10
2.3. BSRN at Cabauw	11
3. Different methods for the determination of sunshine duration	13
3.1. The pyrheliometric method	13
3.2. The pyranometric method	13
3.2.1. The Slob algorithm	14
3.2.2. Adjustments to the Slob algorithm	19
4. Solar radiation measurements	21
4.1. Measurement period	21
4.2. Quality checks	22
4.2.1. Quality flags	22
4.2.2. Ten minute means instead of one minute means	23
5. Comparison of pyrheliometric and pyranometric sunshine duration	27
5.1. Introduction	27
5.2. Daily sunshine duration	28
5.3. Monthly and seasonal sunshine duration	32
5.4. Analysis of the Bergman method in terms of solar elevation angle and cloudiness	34
5.4.1. Solar elevation angle	34
5.4.2. Cloudiness	36
5.5. Conclusions and suggestions for improvement	42
6. Improvement of the pyranometric method	45
6.1. Adjusting the algorithm	45
6.2. Parameterizations and measurements	47
6.3. Sensitivity analysis	50
6.4. A linear algorithm	54
7. Sunshine duration from a sunshine duration sensor	59
7.1. The CSD	59

7.2. Direct irradiance	60
7.3. Sunshine duration determined by the CSD	60
8. Summary and conclusions	65
Acknowledgements	69
Symbols and acronyms	70
References	71

1. Introduction

In this study, the quality of sunshine duration (SD) measurements in the Netherlands is studied. Roughly speaking, sunshine duration is defined as the time during which the sun is visible and it is usually given in hours per day, month, season or year. Sunshine duration measurements have already been performed for over a century (at De Bilt since 1901 (Klimaatatlas, 2002)), in different ways and at many locations around the world. Since long time series of sunshine duration measurements exist, they have a historical value. Sunshine duration is a way to characterise the climate of a particular region (WMO, No 8, 1996), and is used in tourism. Furthermore, if solar radiation measurements are not available, sunshine duration data can give information about the solar radiation, which is valuable for agriculture, architects and solar energy applications (Velds, 1992).

An example of a climatological map of sunshine duration is shown in Figure 1.1. This figure shows the distribution of yearly sunshine duration over the Netherlands, averaged over the period 1971 to 2000. Figure 1.1 clearly shows that the west-coast of the Netherlands receives more sunshine than the eastern part. This is caused by the fact that westerly winds dominate, advecting moist air from sea to land. Over sea there is little convection, but over land the air heats more leading to more convection and more clouds inland. This distribution of sunshine duration will affect, for example, tourism.

Until 1989, the Campbell-Stokes sunshine recorder has been the common instrument to measure the sunshine duration. The first version of this instrument was built by J.F. Campbell in 1853. Adjustments by G.G. Stokes, in 1879, resulted in the Campbell-Stokes recorder (Coulson, 1975). The instrument consists of a glass sphere, mounted concentrically in a section of a spherical bowl, so that the sun's rays are focused on a paper card held in grooves in the bowl. The Campbell-Stokes recorder detects sunshine if the beam solar energy concentrated by a special lens is able to burn a paper card. The card is provided with a time indication, which makes it possible to determine the sunshine duration (in units of 0.1 hour) from the length of the burn when the card is removed from the instrument at the end of the day.

A disadvantage of the Campbell-Stokes recorder is that the determination of sunshine duration is not always accurate, particularly during semi-clouded conditions. Under these weather circumstances dots will be burnt into the card, since sunny periods are alternated by cloudy periods, and the sunshine duration is often overestimated, since it is difficult to determine the

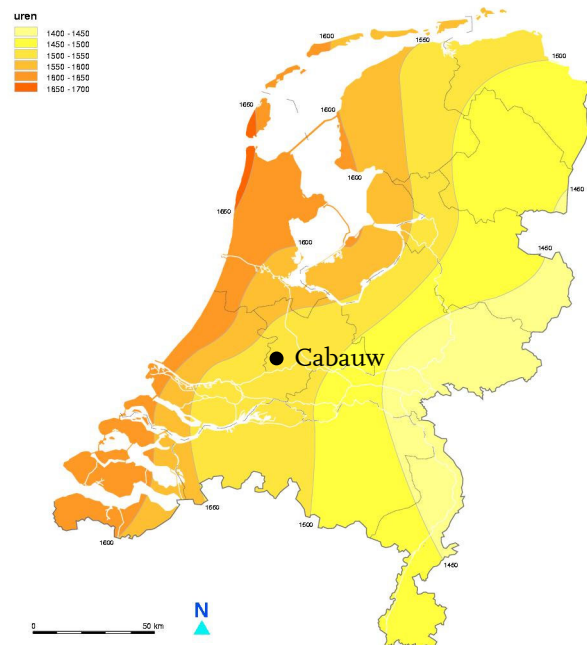


Figure 1.1: Distribution of the yearly sunshine duration (in hours) over the Netherlands averaged over 1971-2000. Yearly averaged sunshine duration over the Netherlands is 1534 h. The black dot indicates the location of Cabauw. (Source: Klimaatatlas van Nederland, KNMI 2002)

exact length of the burn. Furthermore, the morning values can be disturbed by dew or frost, especially at mid and high latitudes.

Despite its inaccuracies, the Campbell-Stokes recorder has been and is used widespread. No international regulations about the exact size and material for the different parts of the instrument were set however, so under the same circumstances different instruments could give different sunshine duration values. This changed in 1962, when the World Meteorological Organization (WMO) recommended the Interim Reference Sunshine Recorder (IRSR), a special design of the Campbell-Stokes recorder, as the standard instrument to measure sunshine duration. The IRSR was set as the standard instrument in order to homogenise the world-wide sunshine duration data during the period needed for finding a precise physical definition, based on measurements of the direct solar irradiance, which could be used in the determination of sunshine duration.

To keep the connection with the Campbell-Stokes recorder, the direct solar irradiance threshold corresponding to the burning threshold of the Campbell-Stokes recorders was studied. Investigations showed that this threshold for burning the card varies between 70 and 280 Wm^{-2} , due to the dependence on humidity (the card will burn more easily under dry conditions than under wet conditions). Further investigations resulted in a mean value for the threshold of 120 Wm^{-2} , which was accepted in 1989 by the WMO as the actual threshold. As a reference sensor for the detection of the threshold irradiance, a pyrheliometer was recommended, an instrument that measures the direct normal solar irradiance (DNSI). Since 1989 the WMO defines sunshine duration officially as the time during which the DNSI exceeds 120 Wm^{-2} . The WMO requirement is that hours of sunshine should be measured with an uncertainty of ± 0.1 hours and a resolution of 0.1 hours (WMO, No 8, 1996). The advantage of this new method is that it is more precise and that it does not involve a burn card that has to be replaced daily, making the new method also applicable at automatic weather stations. Another advantage of the new method is that it involves no burn cards that have to be interpreted manually, which could give rise to different interpretations.

In the Netherlands, the KNMI (Royal Netherlands Meteorological Institute) network of meteorological stations has been automated in the last few decades. Many manned stations now make use of automated observation systems in which the Campbell-Stokes sunshine recorder can no longer be used, since the burn cards have to be replaced manually every day. Furthermore, the new definition of sunshine duration as presented by the WMO presents another reason why the Campbell-Stokes recorder is not suitable for sunshine duration measurements anymore.

According to the WMO definition, DNSI measurements are required to determine the sunshine duration. The DNSI is the radiation from the direction of the sun, measured in a plane perpendicular to the direction to the sun, and it is measured with a pyrheliometer. The pyrheliometer is always pointed towards the sun, which is achieved by a sun tracker. It is an expensive instrument that needs care, which is why the DNSI is only measured at 2 places in the Netherlands. Global radiation on the other hand, is measured at about 30 locations in the Netherlands. Global radiation is measured on a horizontal surface and consists of both the radiation directly from the sun, and the diffuse sky radiation. It is measured with a pyranometer, an instrument that does not require a sun-tracker and is cheaper and needs less care than a pyrheliometer.

If the pyrheliometer would be taken as the standard instrument to determine the sunshine duration, 20 to 30 of these instruments would have to be installed to obtain a representative view of the distribution of sunshine duration over the Netherlands, which is not feasible. Since

pyranometer measurements are already available at about 30 locations, it has been decided to estimate the sunshine duration from global radiation measurements. These estimates are based on an algorithm developed by Slob (Slob and Monna, 1991), which uses the mean, minimum and maximum of the global radiation per 10 minute interval as input and gives the sunshine duration in this interval as output. Slob used the WMO definition for sunshine duration as a reference to develop this algorithm (Slob algorithm). Bergman (1993) made some adjustments to the Slob algorithm to find more agreement with the Campbell-Stokes sunshine duration measurements (Bergman algorithm). This was desirable to guarantee homogeneity of the long time series of Campbell-Stokes sunshine duration measurements that already existed.

Since October 1st 1992 the sunshine duration is operationally determined with the Bergman algorithm at all stations in the Netherlands where the global radiation is measured, and the Campbell-Stokes measurements are no longer used in climatological products.

In this study we will seek for an answer to the following question:

“How well is the quantitative agreement between the sunshine duration determined with the Slob/Bergman algorithm and the “true” sunshine duration, as defined by the WMO, in the Netherlands, and is it possible to increase this agreement by means of improving the Slob/Bergman algorithm?”

The WMO definition of sunshine duration is the accepted definition of sunshine duration in the meteorological world since 1989 and the goal of this research is thus to examine to what extent the sunshine duration as determined in the Netherlands deviates from the sunshine duration as defined by the WMO. For this purpose solar radiation measurements made at the Baseline Surface Radiation Network (BSRN) station in Cabauw are used (Figure 1.1). At this station, global as well as direct normal solar irradiance are measured with high precision and accuracy, enabling a detailed comparison of the different methods. Figure 1.1 indicates that the yearly sunshine duration at Cabauw is close to the yearly average over the country, indicating that, with respect to sunshine duration, Cabauw is a representative location for the Netherlands.

The organization of this report is as follows: First the different radiation instruments are described, in chapter 2. The different methods for the determination of sunshine duration are described in chapter 3. Chapter 4 describes the solar radiation measurements and some quality issues. In chapter 5, the sunshine duration as determined with pyrheliometer measurements is compared to the sunshine duration determined with pyranometer measurements. Chapter 6 investigates the possibility of improving the algorithm used to determine the sunshine duration from pyranometer measurements. In December 2005 a sunshine duration sensor (CSD) was installed at Cabauw, enabling comparison of the sunshine duration determined with this instrument with the sunshine duration derived with the other methods. These results are presented in chapter 7. Finally, the results of this study are summarized in chapter 8, which also presents the conclusions.

2. Instruments for the measurement of solar radiation

As described in the Introduction, there are different methods for determining sunshine duration, all based on different instruments measuring solar radiation. Before giving the instrument details, we first define the radiometric quantity of irradiance (Liou, 2002).

To start with, the monochromatic radiance I_λ is defined:

$$I_\lambda = \frac{dE_\lambda}{\cos(\theta)d\Omega d\lambda dt dA} \quad (2.1)$$

with dE_λ the differential amount of radiant energy in a time interval dt and in a specified wavelength interval λ to $\lambda + d\lambda$, crossing an element of area dA , in directions confined to a differential solid angle $d\Omega$, which is oriented at an angle θ to the normal of dA , so that $\cos(\theta) dA$ denotes the effective area at which the energy is being intercepted. So the intensity is in units of energy per area per time per wavelength and per steradian.

The monochromatic irradiance F_λ (energy per area per time and per wavelength) is now obtained by integrating the normal component of I_λ over the entire hemispheric solar angle:

$$F_\lambda = \int_{\Omega} I_\lambda \cos(\theta) d\Omega \quad (2.2)$$

Then finally, the total solar irradiance F (energy per area per time, expressed in Wm^{-2}) is obtained by integrating the monochromatic irradiance over all wavelengths of the solar spectrum (0.15 to 4.0 μm (Glickman, 2000)):

$$F = \int_{\lambda_1}^{\lambda_2} F_\lambda d\lambda \quad (2.3)$$

with $\lambda_1 = 0.15 \mu\text{m}$ and $\lambda_2 = 4.0 \mu\text{m}$.

In the following section, we describe the instrument used for the WMO definition, the pyrheliometer, and for the Slob/Bergman algorithm, the pyranometer. The first measures direct normal solar irradiance and the second global solar irradiance. The fundamental relationship between the direct normal (I), the global (G) and the diffuse (D) solar irradiance is: $G = I \cos(\theta_o) + D$, where θ_o is the solar zenith angle and $I \cos(\theta_o)$ is the component of I reaching a horizontal surface. We will not further describe the Campbell-Stokes recorder, since the present study will not use measurements made by this instrument. What will be discussed, however, is the BSRN site at Cabauw, where the measurements used in this study are made.

2.1 Pyrheliometer

A pyrheliometer is an instrument which measures the direct normal solar irradiance, integrated over the entire solar spectrum. It is a telescopic type of instrument with a narrow opening called the aperture, as can be seen in Figure 2.1. The receiving surface of the instrument is arranged to be normal to the solar direction, so that only the radiation from the direct solar beam and a

narrow annulus of sky is measured. By mounting the instrument on a solar tracker, it is pointed to the position of the sun automatically.

The instrument should be placed in such a way that the solar beam is not blocked by surrounding obstructions at all times and seasons of the year. Further the optical window must be kept clean, care must be taken that condensation does not appear on the inside, and protection against precipitation is needed.

At Cabauw the Kipp & Zonen CH1 pyrheliometer is used, which covers the total solar spectrum between 200 and 4000 nm (www.kippzonen.com).

2.2 Pyranometer

Pyranometers are used for the measurement of global irradiance, as well as for the measurement of diffuse irradiance.

For the measurement of global irradiance

A pyranometer is an instrument that measures the global irradiance. Global radiation is defined as the solar radiation received from a solid angle of 2π steradian on a horizontal surface (field of view of 180 degrees). A pyranometer is placed horizontally and thus receives radiation directly from the sun as well as diffuse radiation, which has been scattered in the atmosphere.

Like pyrheliometers, pyranometers should be installed on a site as free as possible from obstructions which may shadow the instrument at any time of the year. The pyranometer should not be near to objects that could reflect sunlight onto it or to artificial radiation sources. Further, the glass dome of the instrument should be kept clean and dry.

Both a pyrheliometer and a pyranometer contain a thermopile sensor with a black coating, which absorbs the solar radiation incident on it. This radiation is converted to heat, which flows

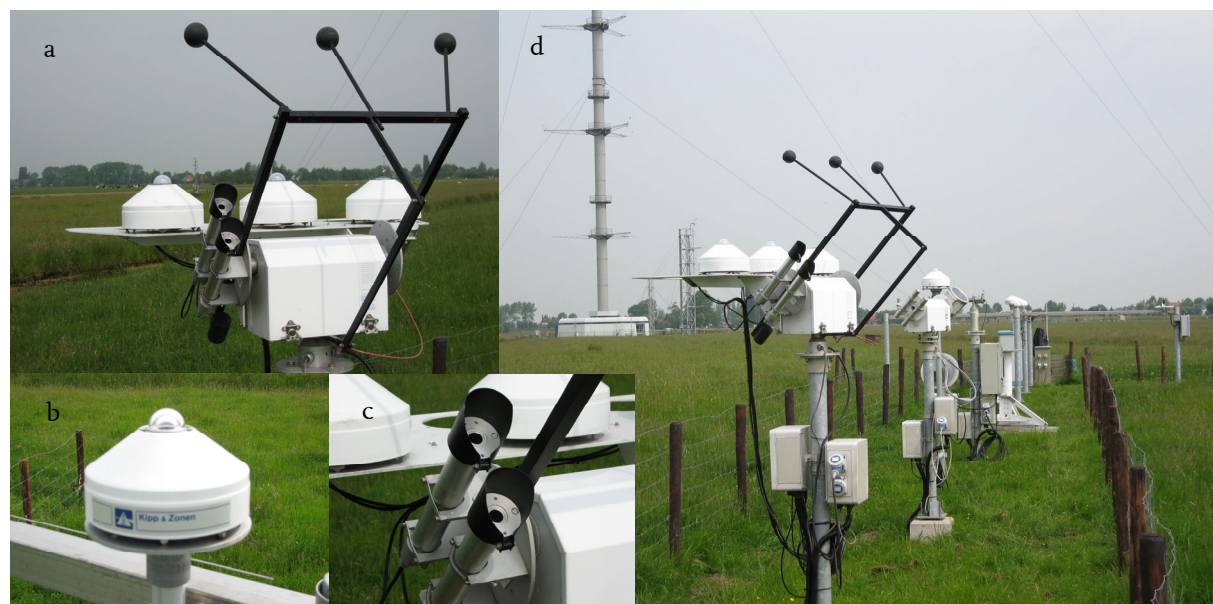


Figure 2.1: Solar radiation instruments at Cabauw: (a) pyrheliometers and shading spheres mounted on a sun-tracker in front of two pyranometers (a CM22 and a CM11) to measure the diffuse radiation, (b) an unshaded pyranometer to measure the global radiation, (c) pyrheliometers for the measurement of direct normal solar irradiance and (d) the BSRN site at Cabauw.

through the sensor to the instrument housing, allowing the thermopile sensor to generate a voltage output signal that is proportional to the solar radiation.

At Cabauw the Kipp & Zonen CM22 ventilated and heated pyranometer is used. The pyranometers that are used in the national network are neither ventilated nor heated (CM 1 1).

For the measurement of diffuse irradiance

The diffuse irradiance is measured with a pyranometer, with a shading device to block the direct solar irradiance. Normally a pyranometer measures the global radiation, but when the direct component is blocked, only the diffuse radiation can reach the instrument. At Cabauw the direct radiation is blocked by a shadow sphere, which is attached to the pyranometer by a thin arm (Figure 2.1). This configuration is mounted on a solar tracker to make sure that the pyranometer is shielded from the direct radiation at all times. Because the shadow sphere is attached to the sun-tracker (on which the pyranometers are mounted) only by a thin arm, almost no diffuse radiation is blocked.

To measure the diffuse radiation at Cabauw, the same type of pyranometer is used as for measuring the global radiation (a Kipp & Zonen CM22 ventilated and heated pyranometer), but with a shading sphere. Figure 2.1 shows a pyranometer both with and without shading sphere.

2.3 BSRN at Cabauw

For this study, radiation measurements from the BSRN station Cabauw (latitude: 51.971 N, longitude: 4.927 E) are used. BSRN is a project of the World Climate Research Programme (WCRP) and the Global Energy and Water Experiment (GEWEX). In 2004 BSRN was designated as the global baseline network for surface radiation for the Global Climate Observing System (GCOS). The understanding of the radiation distribution as provided by the existing radiometric network is not accurate enough to understand the present climate. The simulation of the past and future climate changes, induced by changes in radiation, is even more uncertain. This is why the WCRP initiated BSRN to support the research projects of the WCRP and other scientific programs.

The objective of the BSRN is to provide observations of the best possible quality, for short and longwave surface radiation fluxes, to be able to detect changes in the Earth's radiation field which may be related to climate change. Currently these readings are taken from 35 BSRN stations in contrasting climatic zones, together with collocated surface and upper-air meteorological data. The data are particularly important for the validation and confirmation of satellite and computer model estimates of these quantities.

Cabauw is a BSRN station, meaning that radiation measurements are made with the BSRN standard accuracy. The BSRN accuracy requirements are based on the accuracy considered necessary by the satellite and model communities for validating satellite-based estimates of the surface radiation budget and improvement of radiation codes of climate models (Ohmura et al., 1998). Achieving the highest irradiance accuracy requires a high sampling frequency (1 Hz) and short archival interval (1 min). The Cabauw site is chosen for the present analysis of sunshine duration because it includes a pyrhelimeter, a pyranometer and a shadowed pyranometer, so that the direct normal, global as well as the diffuse solar irradiance are measured, which is unique for the Netherlands. The measurements of DNSI are needed to determine the sunshine duration according to the WMO definition, while the global irradiance measurements can be used to

determine the sunshine duration with the Slob or Bergman algorithm. The measurements of the diffuse component are also useful, since they can be used to check the relationships that are used for the algorithms.

All instruments have a sampling rate of 1 Hz. This means that every second the measurement can be compared to the WMO threshold of 120 Wm^{-2} and sunshine seconds can be determined.

The data acquisition system of the national network stores 10 minute means and extremes based on 12 s readings of the global irradiance. To guarantee agreement with the original design of the algorithm, this resolution is also used in this study, so not all measurements of the global irradiance are used to determine the mean, minimum and maximum of the global irradiance in a 10 minute interval, but only 1 measurement every 12 seconds.

3. Different methods for the determination of sunshine duration

In this study different methods for the determination of sunshine duration are compared. The main methods are the pyr heliometric method (based on measurements of direct irradiance) and the pyranometric method (based on measurements of global irradiance). The pyranometric method exists in different variations, since both Bergman and Schipper made some adjustments to the original Slob algorithm, which is used in the pyranometric method.

3.1 The pyr heliometric method

The pyr heliometric method is based on the sunshine duration according to the WMO definition. The WMO CIMO Guide No. 8 (1996) states that “the sunshine duration during a given period is defined as the sum of that subperiod for which the direct solar irradiance exceeds 120 Wm^{-2} ” and that “hours of sunshine should be measured with an uncertainty of ± 0.1 hours and a resolution of 0.1 hours”.

In the present study, the pyr heliometric method is based on measurements of the DNSI per second and the WMO threshold of 120 Wm^{-2} . If the measured value exceeds this threshold, this second is determined as sunny. Since this method uses measurements of the direct radiation, we call it the Direct method. The corresponding sunshine duration is given the symbol SD_{Direct} and is considered to be the true sunshine duration. It should be noted that the Direct method deviates from the WMO definition, because it uses one measurements per second, and the WMO definition only requires a resolution of 0.1 hours. Earlier, this high sampling rate of DNSI measurements was used by Forgan and Dyson (2003, 2004), who determined the sunshine seconds in a minute. These authors assessed the uncertainty in daily sunshine duration from BSRN minute statistics for measurements in the Australian Network.

The response time of the pyr heliometer is 7 s (95% level), which means that the instrument does not respond instantaneously. However, since the sampling time (1 s) is much less than the response time (7 s), no information is lost in the pyr heliometric direct irradiance signal (Forgan, personal communication).

3.2 The pyranometric method

The pyranometric method is based on measurements of the global radiation, as made by a pyranometer.

The relation between global radiation and sunshine duration has been studied extensively. For the Netherlands, this relation was for example studied by Frantzen and Raaff (1982), but it has also been studied for other parts of the world (see for example Gopinathan (1988), Al-Sadah and Ragab (1991), Hussain *et al.* (1999), El-Metwally (2005)). In most of these studies it is attempted to estimate the global radiation from sunshine duration measurements (i.e. the reverse problem of this study). This is done, because in many countries sunshine duration is measured (mostly with Campbell-Stokes recorders) at more locations than the global radiation. Knowledge of the global radiation is desired for the design and prediction of systems which use solar energy.

Since solar radiation data is not available for all locations where solar energy devices may be used, different correlations between global radiation and sunshine duration have been suggested.

Ångström was the first to propose an empirical relation estimating the monthly mean daily global radiation on a horizontal surface (Ångström, 1924; Iqbal, 1983). The Ångström-Prescott relation (Iqbal (1983), and references therein) is a slightly adjusted form of this empirical relation, linearly relating the monthly mean daily global radiation on a horizontal surface to the relative sunshine duration. The exact form of this relation depends on the location and climate, but, once derived, it may be used for locations with similar climatological and geographical characteristics at which solar data is not available.

Many other correlations relating global radiation to sunshine have been suggested, station dependent as well as station independent, linear or non-linear, taking into account for example latitude, elevation, atmospheric water vapour concentration, cloud cover or temperature, beside sunshine duration. However, the Ångström-Prescott relation has been found to be widely applicable in determining global solar radiation for different locations around the world. This relation thus estimates the global radiation from sunshine duration measurements, while for the Netherlands, Slob and Monna (1991) attempted the opposite: the determination of sunshine duration from global radiation measurements. Besides, the Ångström-Prescott equation is valid for monthly means, while Slob and Monna proposed to estimate the sunshine duration per 10 minute interval, to obtain realistic estimates of the sunshine duration also during the day. For this purpose Slob and Monna developed an algorithm for estimating the sunshine duration from the mean, minimum and maximum of global radiation in a 10 minute interval. The pyranometric method that uses this algorithm to determine the sunshine duration is referred to as the Slob method and the sunshine duration determined with this method is given the symbol SD_{Slob} .

3.2.1 The Slob algorithm

In what follows, we will describe the Slob algorithm. First the parameterization of different radiation components is discussed, which will then be used in the description of the actual algorithm. The algorithm is separated into different solar elevation angle intervals and will be discussed according to this division.

Parameterization of radiation components

In the Earth's atmosphere, radiation is partly absorbed and scattered by air molecules, clouds and other particles in the atmosphere. The radiation that reaches the surface consists of a direct normal component (I) from the direction of the sun and a diffuse component (D) from all other directions. The global radiation (G) on a horizontal surface is partitioned into a direct and diffuse component:

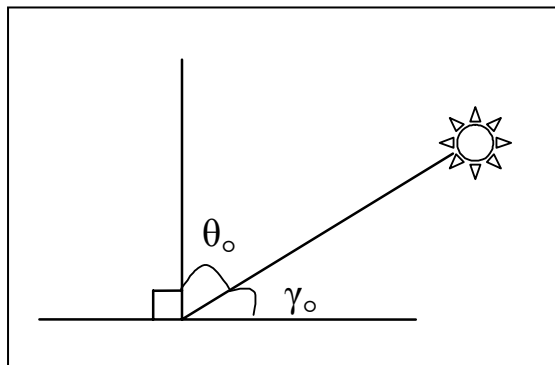


Figure 3.1: Solar zenith angle (θ_0) and solar elevation angle (γ_0).

$$G = \mu_0 I + D \quad (3.1)$$

Where $\mu_0 = \cos(\theta_0) = \sin(\gamma_0)$, in which θ_0 is the solar zenith angle. For convenience, we also define the solar elevation angle (γ_0 ; Figure 3.1). $\mu_0 I$ is the

contribution of the direct radiation on a horizontal surface and D is the diffuse radiation on a horizontal surface.

The basis of the Slob algorithm is the estimation of the direct and diffuse radiation for cloudless conditions:

$$I = I_o \exp\{-T_L / (0.9 + 9.4\mu_o)\} \quad (3.2)$$

$$D = 40.3 + 41.3\mu_o T_L \quad (T_L < 12.5; 0.087 < \mu_o < 0.87) \quad (3.3)$$

These estimates are based on a three year dataset (May 1986 to May 1989) of 10 minute means of I, D and G as well as the minimum and maximum values of G for each 10 minute interval. For the development of the sunshine duration algorithm itself, Slob used a dataset for the period October 1989 to April 1990. Measurements of the 10-minute mean direct irradiance were used as a reference for the sunshine duration estimation, using the WMO definition of sunshine duration.

For the estimation of the direct irradiance for cloudless conditions (Equation (3.2)) the parameterization of Kasten (1980) is used. This parameterization takes into account both turbidity (T_L) and solar elevation (μ_o). The direct radiation reaching the ground, will depend on the solar elevation angle, because the higher the elevation of the sun above the horizon, the shorter the path length of the radiation through the atmosphere. If the path length is shorter, less absorption and scattering will take place in the atmosphere, and the direct radiation at the surface is what is left of the top of the atmosphere irradiance after scattering and absorption in the atmosphere. The Linke turbidity factor, T_L (Linke, 1922), is a measure of the attenuation of solar radiation through extinction by aerosols and water vapour in the atmosphere. This is a dimensionless quantity, which represents the impact of the true atmosphere on radiation with respect to a clean and dry atmosphere without trace gases and aerosols. Equation (3.2) shows that a higher turbidity leads to less direct radiation at the surface.

I_o (in Equation (3.2)) is the solar irradiance at the actual Earth-Sun distance. The solar constant is the solar irradiance at mean Earth-Sun distance on a surface perpendicular to the solar beam and integrated over the whole spectrum, and equals 1366 Wm^{-2} (Liou, 2002). At the mean Earth-Sun distance I_o thus equals the solar constant, while it can vary from this value by about 3.5% due to the elliptical orbit of the Earth around the Sun. This effect is taken into account in the algorithm.

For the diffuse irradiance (Equation (3.3)), the Linke turbidity factor and the solar elevation angle are also the most important parameters. A simple relationship between D, T_L and μ_o is assumed, in which D is proportional to $\mu_o T_L$. By means of linear regression, Slob found the expression given in Equation (3.3) for the diffuse component for cloudless periods between May 1986 and May 1988.

Since I_o and μ_o are known for a given situation, (3.1), (3.2) and (3.3) show that when also T_L is known, D and I can be determined from a measurement of the global radiation.

In the algorithm I, D and G will be normalised with G_o , which is the radiation on a horizontal surface, outside the atmosphere:

$$G_o = \mu_o I_o \quad (3.4)$$

An advantage of this dimensionless form is the – to a first approximation – independence of μ_o , so that values from different times and different seasons can be easily compared. Some

dependence on μ_o is still present though, because of the relationship between μ_o and the path length through the atmosphere.

Separation into μ_o -intervals

In this subsection, the actual algorithm will be explained. The structure of the Slob algorithm is given in Figure 3.2.

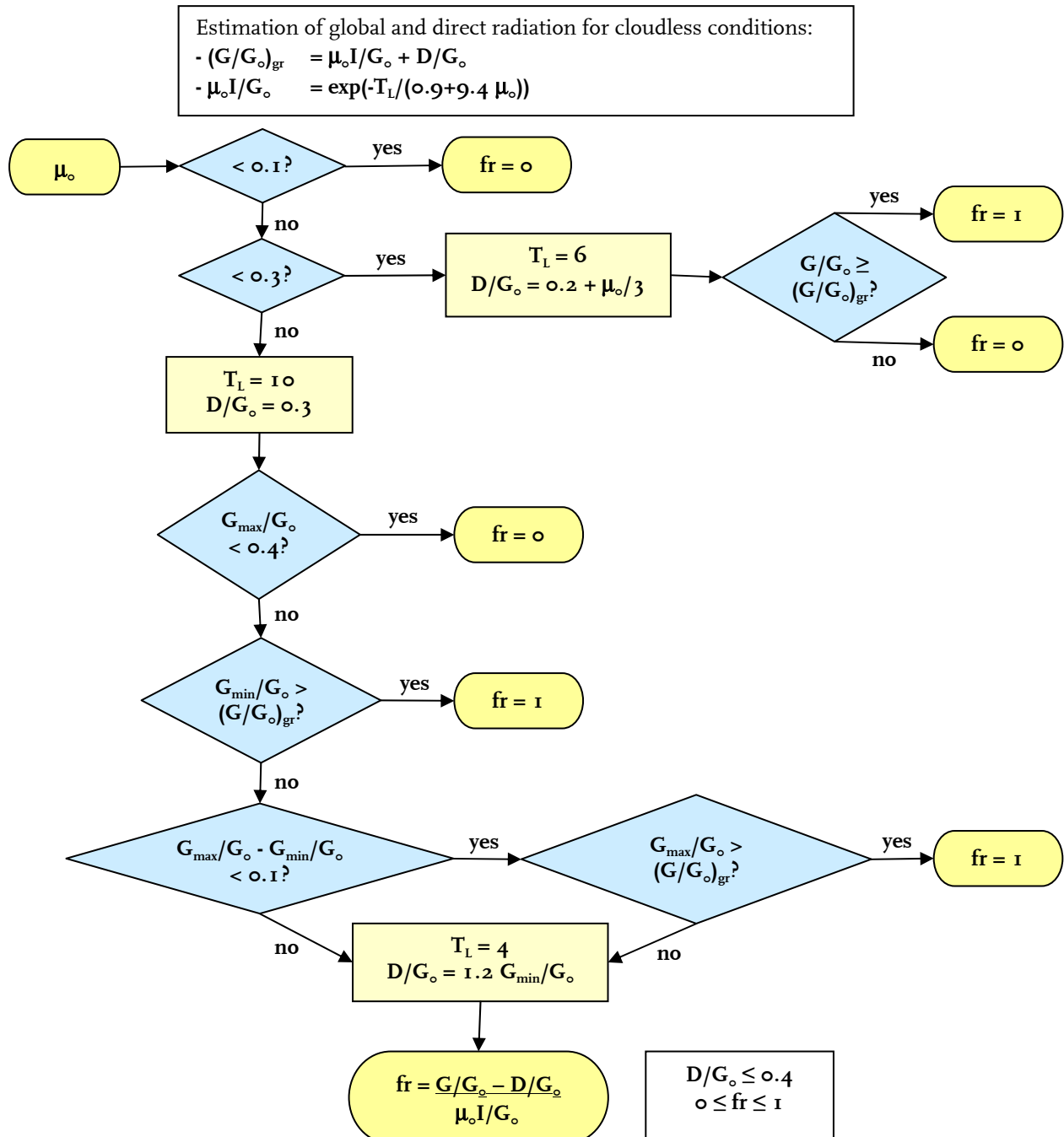


Figure 3.2: The Slob algorithm.

When applying the algorithm, first the global irradiance under cloudless conditions, $(G/G_o)_{gr}$, as given in the box at the top of Figure 3.2, should be considered. This involves an estimation of the direct and diffuse irradiance under clear skies. The direct irradiance is estimated by the

parameterization of Kasten, and depends on μ_o and the Linke turbidity factor T_L , which varies for the different μ_o -intervals. After considering the box in Figure 3.2, the flowchart itself can be applied. Per 10 minute interval a choice is now made depending on the value of μ_o and the flowchart is followed in a specific direction until a value for the fraction of sunshine (fr) has been found for this 10 minute interval, after which the next 10 minute interval can be considered. This way the algorithm can be applied to all 10 minute intervals of interest and of these 10 minute values of sunshine duration daily totals can be computed, for example.

As shown in Figure 3.2, the algorithm distinguishes between different solar elevations. In the following, each μ_o interval will be discussed in more detail.

$\mu_o < 0.1$ ($\gamma_o < 5.7^\circ$) The fraction of sunshine is set to zero. This is done because the irradiance reaching the ground is reduced by the atmosphere to such an extent that the threshold $I = 120 \text{ Wm}^{-2}$ will only be reached under very clear skies. Besides, these elevation angles only occur for a short time of the day. The contribution of these elevation angles to the sunshine duration will thus be small, and is therefore neglected in the algorithm.

$0.1 \leq \mu_o < 0.3$ ($5.7^\circ \leq \gamma_o < 17.5^\circ$) The algorithm distinguishes between completely cloudy or completely sunny situations. This is quite a crude approximation, because within 10 minutes there can be a cloudy period next to some sunshine minutes. Slob chose this division, because it is difficult to classify the different situations at these elevation angles. In summer, for example, the elevation angle increases rapidly during sunrise, resulting in large differences between the minimum and maximum value of the global radiation within 10 minutes. Further, clouds can be illuminated from below, giving rise to a high value for the diffuse irradiance. This increases the global radiation, making it difficult to distinguish between a sunny and a partly cloudy sky.

In the algorithm, a value for the global irradiance under cloudless conditions $(G/G_o)_{gr}$ is estimated. If the measured normalised global irradiance (G/G_o) exceeds this limit, it is assumed that the interval was completely sunny.

Slob and Monna used radiation measurements from October 1989 to April 1990 to obtain the following estimate of D/G_o :

$$D/G_o = 0.2 + \mu_o / 3 \quad (3.5)$$

Equation (3.5) differs from Equation (3.3), but is not in disagreement with (3.3). Equation (3.3) is fitted to data with γ_o between 5° and 60° , while (3.5) is only valid up to 17.5° . For small elevation angles D/G_o increases with μ_o , but averaged over all angles, D/G_o decreases slightly with μ_o .

For these μ_o , $T_L = 6$ is taken as mean atmospheric turbidity and the parameterization of Kasten is used to estimate the direct irradiance. Then I is multiplied by μ_o to obtain the direct irradiance on a horizontal surface instead of on a surface perpendicular to the direction of the sun:

$$\mu_o I / G_o = \exp\{-T_L / (0.9 + 9.4\mu_o)\} \quad (3.6)$$

With (3.1), the estimation of the global irradiance for cloudless conditions becomes:

$$(G/G_o)_{gr} = \mu_o I / G_o + D/G_o \quad (3.7)$$

And the fraction (*fr*) of sunshine duration in each 10 minute interval is given by:

$$G/G_o \geq (G/G_o)_{gr} \rightarrow fr = 1 \quad (\text{completely sunny}) \quad (3.8a)$$

$$G/G_o < (G/G_o)_{gr} \rightarrow fr = 0 \quad (\text{completely cloudy}) \quad (3.8b)$$

The sunshine duration in minutes per 10 minute interval is achieved by multiplying the fraction by ten.

$\mu_o \geq 0.3$ ($\gamma_o \geq 17.5^\circ$) The situations cloudy, sunny and partly cloudy are distinguished. A situation is said to be completely cloudy if $G_{max}/G_o < 0.4$, in which G_{max} is the maximum measured value of the global radiation in the 10 minute interval. Slob found the value of $G_{max}/G_o = 0.4$ to be an upper limit for cloudy situations, since measurements showed that the direct irradiance vanishes below this value. Completely cloudy periods can thus be recognised by:

$$G_{max} / G_o < 0.4 \rightarrow fr = 0 \quad (\text{completely cloudy}) \quad (3.9)$$

To recognise completely sunny periods $D/G_o = 0.3$ is assumed.¹ Again an estimation of the global irradiance is made with Equations (3.6) and (3.7), but now $T_L = 10$ is chosen. In general this gives a limit $(G/G_o)_{gr}$ that can only be exceeded when there is direct radiation. So when $G_{max}/G_o > (G/G_o)_{gr}$ there was direct radiation in the 10 minute interval. When also G_{min}/G_o is larger than the limiting value $(G/G_o)_{gr}$, direct radiation was present continuously and the period is said to be completely sunny:

$$G_{min} / G_o > (G/G_o)_{gr} \rightarrow fr = 1 \quad (\text{completely sunny}) \quad (3.10)$$

Only in situations with much diffuse radiation, possibly in combination with some direct radiation this test does not work; then the global irradiance will be high and $fr = 1$ is found, even though there is hardly any direct radiation.

The period is also determined as completely sunny when G_{max}/G_o exceeds the limit $(G/G_o)_{gr}$ and the difference between G_{max} and G_{min} is small, so when the following variability criterion is met:

$$G_{max} / G_o > (G/G_o)_{gr} \text{ and } (G_{max} / G_o - G_{min} / G_o) < 0.1 \rightarrow fr = 1 \quad (3.11)$$

(completely sunny)

Large differences between G_{min} and G_{max} are an indication for the presence of clouds. When a cloud is in front of the sun, the direct radiation is blocked and the global radiation will decrease compared to the situation where the sun is visible. In the case of broken clouds there will also be periods during which the sun is visible, meaning that the global radiation will increase again. If this happens within 10 minutes, the differences between G_{min} and G_{max} can become quite large. And even if the sky stays cloudy within a 10 minute interval, the differences between G_{min} and G_{max} can still be larger than under clear skies, because the thickness of the clouds can vary.

¹ This value for D/G_o can be approximated from Equation (3.3): with $I_o = 1366 \text{ Wm}^{-2}$ and $T_L = 10$, D/G_o lies between 0.3 and 0.4.

When G_{\max}/G_o is larger than $(G/G_o)_{gr}$, but the differences between G_{\min}/G_o and G_{\max}/G_o are larger than 0.1, it is likely that there are clouds. It is possible though that these are broken clouds, so that only part of the 10 minute interval is cloudy and part is sunny. These situations are the last to contribute to the sunshine duration and are dealt with in the last part of the algorithm. D/G_o is now given as a function of G_{\min} (derived from measurements used by Slob and Monna):

$$D/G_o = 1.2G_{\min}/G_o \quad (3.12)$$

where D/G_o is set to 0.4 when $1.2G_{\min}/G_o \geq 0.4$

D/G_o is a function of G_{\min} , because when a cloud obscures the sun the direct radiation vanishes, D will equal G and G will reach its minimum value G_{\min} . This means that D equals G_{\min} when a cloud is in front of the sun. D will be a little larger when this cloud is not in front, but just next to the sun, because reflection at this cloud can then contribute to the diffuse radiation.

D/G_o is bounded at 0.4, because larger values would mark situations with direct radiation but relatively much diffuse radiation as cloudy, while there was possibly some sunshine.

The fraction of sunshine duration is now estimated by dividing the true value of the direct irradiance by the value of the direct irradiance in case the sun would have shone continuously (Equation (3.6)). The true value is estimated by subtracting the estimated value for the diffuse irradiance (Equation (3.12)) from the measured global irradiance:

$$fr = \frac{(G/G_o - D/G_o)}{\mu_o I / G_o} \quad \text{where } 0 \leq fr \leq 1 \quad (\text{broken clouds}) \quad (3.13)$$

The fraction sunshine has to lie between 0 and 1 by definition, therefore fr is set to zero when $fr < 0$ and to one if $fr > 1$. In this last part the relatively low value of $T_L = 4$ is chosen to correct for the fact that all periods with direct irradiance count in estimating the sunshine duration, even when the DNSI is actually smaller than 120 Wm^{-2} .

Slob compared the results from his algorithm to the sunshine duration determined from measurements of the direct irradiance. He concluded that the accuracy of sunshine duration determined with the algorithm is comparable to the accuracy of Campbell-Stokes measurement of sunshine duration and is of the order ± 0.6 hours for daily totals.

3.2.2 Adjustments to the Slob algorithm

After the Slob algorithm was developed, it was studied and adjusted by both Bergman (1993) and Schipper (2004). The Bergman algorithm is operationally in use by the KNMI to determine the sunshine duration. The Schipper algorithm has never been operationally used, but both adjustments to the original algorithm will be shortly discussed here.

Bergman

The method that uses the Slob algorithm as adjusted by Bergman for the determination of the sunshine duration is a second example of a pyranometric method, and will be referred to as the Bergman method. This method does not differ from the Slob method very much. It also uses an algorithm to estimate the sunshine duration in a 10 minute interval when the mean, minimum and maximum of the global irradiance are given. The only difference lies in the algorithm itself.

Bergman made some adjustments to the Slob algorithm to find more agreement with the Campbell-Stokes measurements. This was done because a long time series of Campbell-Stokes sunshine duration measurements already exists and it was desirable to guarantee homogeneity.

The adjustments Bergman made are:

- (a) Minimal solar elevation γ_0 that contributes to the sunshine duration corresponds to $\mu_0 = 0.05$ in stead of $\mu_0 = 0.1$.
- (b) The interval $0.05 \leq \mu_0 < 0.3$ is split in two: $0.05 \leq \mu_0 \leq 0.087$ with $T_L = 3.5$ and $0.087 < \mu_0 < 0.3$ with $T_L = 6$.
- (c) For $\mu_0 \geq 0.3$ and partly cloudy conditions, $T_L = 8$ is chosen in stead of $T_L = 4$.

These adjustments mainly concern the solar elevation angles that can possibly contribute to the sunshine duration. In the original Slob algorithm only the times when the sun was more than 5.7° above the horizon could add to the sunshine duration. Bergman lowered this limit to 2.9° , so that the contribution from times when the sun is low in the sky is also taken into account.

The adjustments Bergman made to the algorithm are based on a statistical comparison of sunshine duration calculations with parallel Campbell-Stokes measurements during the period May 1991 to December 1991 on 3 different locations (De Bilt, Wilhelminadorp and Hupsel/Winterswijk) (Bergman, 1993).

Schipper

The third variation of a pyranometric method uses the algorithm developed by Slob, but with the adjustments of Schipper (2004), and is therefore called the Schipper method.

Schipper used a dataset of 10 minute means, minima and maxima of the global irradiance from January 1995 to December 2002. Further also pyrhelimetric measurements of the DNSI and measurements of a Campbell-Stokes sunshine recorder were used. This allowed Schipper to compare the sunshine duration as estimated with the Slob and Bergman method to each other, but also to the sunshine duration as determined directly from the DNSI measurements (pyrhelimetric method) and to the sunshine duration as given by the Campbell-Stokes recorder.

The sunshine duration as derived with the Slob method as well as that derived with the Bergman method differs from that derived with the Direct method. For the development of the Slob algorithm and also for the adjustments Bergman made to the algorithm, only a short dataset was used. Schipper used a longer dataset to adjust the parameterizations used in the algorithm through means of linear regression analysis.

The adjustments Schipper made to the Slob algorithm are:

- (a) Minimal solar elevation γ_0 that contributes to the sunshine duration corresponds to $\mu_0 = 0.05$ in stead of $\mu_0 = 0.1$.
- (b) The interval $0.05 \leq \mu_0 < 0.3$ is split in two: $0.05 \leq \mu_0 \leq 0.087$ with $T_L = 2.25$ and $0.087 < \mu_0 < 0.3$ with $T_L = 3.24$.
- (c) For the interval $0.05 \leq \mu_0 < 0.3$, the diffuse radiation under cloudless conditions is estimated by $D/G_0 = 0.17 + 0.17 \mu_0$.
- (d) For $\mu_0 \geq 0.3$ and cloudless conditions $T_L = 4.36$ and $D/G_0 = 0.22$, while for partly cloudy conditions, $T_L = 13.03$ and $D/G_0 = 1.27 G_{\min}/G_0$.

Although the Schipper algorithm is based on a longer dataset than the Bergman algorithm, the Bergman algorithm is still used by the KNMI to determine the sunshine duration for climatological purposes.

4. Solar radiation measurements

In the previous sections different methods for the determination of the sunshine duration have been discussed, as well as the instruments needed to make the measurements for the application of these methods. In this section we will describe the radiation measurements used for the analysis of sunshine duration. Furthermore, we will discuss the quality of the measurements according to specific BSRN procedures.

4.1 Measurement period

The construction of the BSRN site was completed by the end of 2004 and first measurements became available in January 2005. These first measurements, however, were not used for the present analysis, because of start-up problems. In order to consider a full year of measurements, data for the period March 2005 – February 2006 are used for the analysis of sunshine duration presented here.

Some data could not be used, because of problems with the data acquisition system, power loss or sun-tracking problems. During the year, problems occurred on 41 days (13 days in spring, 7 in summer, 13 in autumn and 8 in winter). The data of the days on which problems occurred are given in Table 4.1. Measurements made on these days will not be used in the analysis.

Table 4.1: Days on which problems occurred. The data for these days are omitted from the analysis.

Date	Daynumber	Reason for omitting data
27-29 Mar	86-88	Error in time because of summertime
7 Apr	97	Data incomplete (replacement SIAMs)
26 Apr	116	Data incomplete (working activities)
28-29 Apr	118-119	Data incomplete (power loss)
30 Apr-4 May	120-124	Problems with data acquisition system (problems with SIAM)
11 May	131	Sun-tracker off track
20 Jun	171	Problems with SIAM because of heat
23-24 Jun	174-175	Problems because of heat
14 Jul	195	Replacement of pyranometer (CM22) (to try to suppress restterm)
7 Aug	219	Sun-tracker off track
22-23 Aug	234-235	Problems with data acquisition system
1-5 Sep	244-248	Sun-tracker off track (due to bird of prey)
28 Sep-3 Oct	271-276	Sun-tracker off track
23-24 Nov	327-328	Data incomplete (problems with data acquisition system)
3-5 Dec	337-339	Data incomplete (problems with data acquisition system)
6 & 8 Dec	340 & 342	Data incomplete (due to sound campaign)
29 Dec	363	Sun-tracker off track
13 Jan	13	Unknown
8 Feb	39	Problems with data acquisition system

4.2 Quality checks

Before using the data of the different radiation instruments for the analysis, the quality of the data is checked. This is done to make sure that differences in sunshine duration between the different methods are not caused by measurement errors.

4.2.1 Quality flags

Long and Dutton (scientists of the BSRN community) developed quality control procedures in order to flag radiation data suspected of being erroneous. For the present study, the quality is checked by means of three quality checks: the first concerning physically possible limits of the radiation measurements, the second concerning extremely rare limits and the third concerning ratios of different radiation components. These quality checks are based on experience, empirical relations and model calculations. A diffuse irradiance larger than 700 Wm^{-2} has, for example, never been measured yet. And on the other hand, model calculations with a Rayleigh atmosphere provide the minimum possible value for the diffuse irradiance, since aerosols will scatter radiation thereby increasing the diffuse radiation.

For the quality checks, 10 minute mean values of I , G , D and μ_0 are used. For the computation of the position of the sun (μ_0) at Cabauw the Astronomical Almanac's Algorithm is used (Michalsky, 1988).

Physically possible limits (PPL) & extremely rare limits (ERL): If the value for G , D or I is not between the minimum and maximum as specified in Table 4.2, this measurement is flagged with the value that is mentioned in the last column of Table 4.2. If the values are between the minimum and the maximum, then the flag is given the value zero, meaning that the quality of the data is good.

Ratios: Like for the physically possible and extremely rare limit checks the values are also flagged according to the ratios (Table 4.3). If the ratio condition is met (ratios between min and max) then this flag is set to zero, otherwise the value as specified in the last column of Table 4.3 is given to the flag.

These checks are performed on every 10 minute interval, leaving every interval with a PPL, an ERL and a ratios-flag. For the analysis presented here, all data for which one of the flags does not equal zero were omitted, so only data of good quality are used for the analysis of sunshine duration.

Table 4.2: Physically possible limits and extremely rare limits– check (Long and Dutton, BSRN Global Network recommended QC tests, V2.0).

Parameter	Minimum (Wm^{-2})	Maximum (Wm^{-2})	Flag
<i>Physically possible limits – check</i>			
G	-4	$1.5 I_0 \mu_0^{1.2} + 100$	1
D	-4	$0.95 I_0 \mu_0^{1.2} + 50$	2
I	-4	I_0	4
<i>Extremely rare limits – check</i>			
G	-2	$1.2 I_0 \mu_0^{1.2} + 50$	1
D	-2	$0.75 I_0 \mu_0^{1.2} + 30$	2
I	-2	$0.95 I_0 \mu_0^{0.2} + 10$	4

Table 4.3: Ratios – check: $Ratio = G/(\mu_o I + D)$; $Ratio_dif = D/G$; $Sum = \mu_o I + D$.

Parameter	Minimum	Maximum	Restriction to data	Flag
Ratio	0.92	1.08	$\theta_o < 75^\circ$ and $Sum > 50 \text{ Wm}^{-2}$	1
Ratio	0.85	1.15	$75^\circ < \theta_o < 93^\circ$ and $Sum > 50 \text{ Wm}^{-2}$	2
Ratio_dif	-	1.05	$\theta_o < 75^\circ$ and $G > 50 \text{ Wm}^{-2}$	4
Ratio_dif	-	1.10	$75^\circ < \theta_o < 93^\circ$ and $G > 50 \text{ Wm}^{-2}$	8

The effect of the quality checks on the data can be seen by plotting $\mu_o I + D$ against G (Figure 4.1). Measurements for which all flags are zero are plotted in black, while measurements for which one of the flags is not zero are plotted in red. Most points are expected near the line $\mu_o I + D = G$, because this is the actual relation between the radiation components. Figure 4.1 indeed shows that most points that are not on the line $\mu_o I + D = G$ turn red and will be omitted in the analysis.

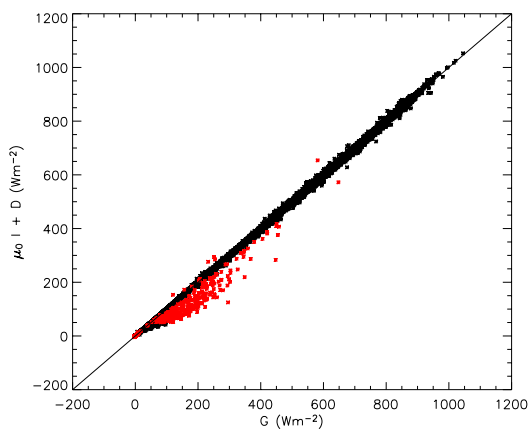


Figure 4.1: Quality check: $\mu_o I + D$ against G , both in Wm^{-2} . The red points indicate data for which one of the quality flags is not equal to zero. Data from March 2005 to February 2006 is used.

For the period March 2005 – February 2006, 1.1% of the 10 minute intervals do not meet the quality requirements.

For small irradiances, some black points can be found off the line $\mu_o I + D = G$ in Figure 4.1. It appeared that these points correspond to periods during which the DNSI measured by the pyrheliometer is too low, due to the presence of condense on the windows of the pyrheliometer. This happened in particular during spring and autumn mornings ($\mu_o < 0.2$). Since the irradiances are low during the times when condense is present, the sunshine duration will be hardly affected by it, the data associated with these periods are not omitted from the dataset.

4.2.2 Ten minute means instead of one minute means

Originally the quality flags were determined for 1 minute mean values of G , D , I and μ_o . In the present study 10 minute means are used in stead of 1 minute means. The reason for this lies in the movement of the pyranometer on July 14th 2005.

Before July 14th the pyranometer was placed rather far from the pyrheliometer (~15 m). During periods that were partly cloudy, it could be the case that the pyrheliometer was placed in the sun, while the pyranometer was in a shaded area. When this occurs, the pyrheliometer receives direct irradiance, while the pyranometer does not. The sum of the direct and diffuse irradiance will then differ significantly from the measured global radiation, and the ratio $G/(\mu_o I + D)$ will not lie between the minimum and the maximum values specified in Table 4.3. Minutes during which this occurs are therefore flagged unequal to zero, even though there is no measurement error and these data are suitable for sunshine duration determination. On July 14th the pyranometer was moved, and placed closer to the pyrheliometer, so this problem would no longer occur and the pyranometer and pyrheliometer would be either both in the shade or both in the sun.

After July 14th one minute means of G, D and I can thus be used to determine the quality flags, but before July 14th this leads to some flagging during periods with broken clouds. The idea now is that within a 10 minute interval however, the pyranometer and pyrliometer will be shaded during an approximately equal part of the interval, due to the movement of the clouds. Using 10 minute mean values of G, D and I for the quality flags might thus solve the problem of the flagging. Whether this is the case, is checked by looking at days with broken clouds before and after July 14th and determining the flags on basis of 1 minute means as well as on basis of 10 minute means. As an example July 7th and August 11th are chosen. Figure 4.2 shows the radiation components G, D and I as measured on July 7th and August 11th 2005 at Cabauw as a function of time. July 7th and August 11th are both days with broken clouds, as shown by the large variations in the direct irradiance in Figure 4.2, indicating that the sun is visible at one instant (direct irradiance > 0) and behind a cloud a little later (no direct irradiance). In Figure 4.3 and Figure 4.4 the ratio $G/(\mu_0 I + D)$ is plotted as a function of time during the day for July 7th and August 11th, respectively. The left images show this ratio on basis of minute means, while the right images show the same ratio on basis of 10 minute means of G, D and I. The dotted lines in the figures indicate the ratio-limits, between which the ratio-flag for the period is given the value zero.

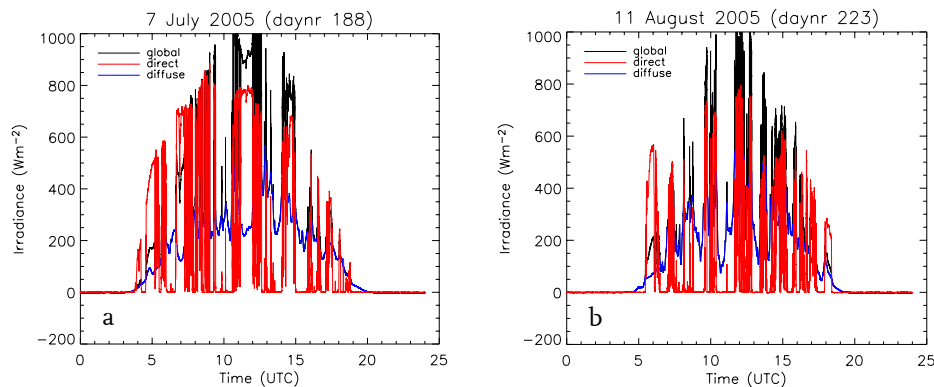


Figure 4.2: Measurements (in Wm^{-2}) of the direct normal (red), diffuse (blue) and global irradiance (black) as a function of time (UTC) during the day. (a) On 7 July 2005 and (b) on 11 August 2005.

Figure 4.3 gives the situation before the movement of the pyranometer. When minute mean values are used to determine the ratios, the ratio-limits are crossed several times on this day, while the ratio-limits are not crossed at all when 10 minute means are used. Figure 4.4 gives the situation after the movement of the pyranometer. The radiation components on August 11th are comparable with those on July 7th, but for August 11th the ratio-limits are not crossed, whether minute or 10 minute means are used for the ratios. This indicates that the movement of the pyranometer had the desired effect, and that the data is no longer erroneously flagged unequal to zero after July 14th.

From Figure 4.3 it can also be concluded that, using 10 minute means for D, G and I in stead of 1 minute means, lowers the ratios, so that the ratio-limits are not so easily crossed. Measurements that would have been given a flag unequal to zero with the use of minute means are correctly flagged zero when 10 minute means are used. Using 10 minute means for G, D, I and μ_0 in the quality checks in stead of minute means is thus a good solution to get round the problem of the flagging. To make fair comparisons, these 10 minute means will be used for the analysis presented in this report.

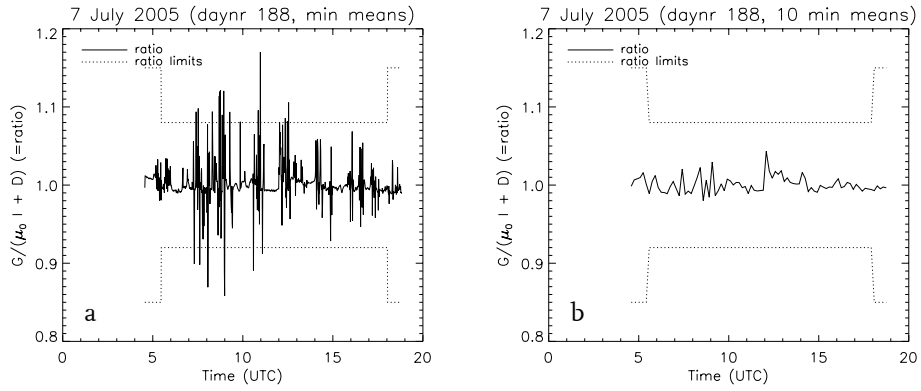


Figure 4.3: The ratio $G/(\mu_0 I + D)$ (a) on the basis of minute means and (b) on the basis of 10 minute means as a function of time (UTC) for 7 July 2005. The dotted lines indicate the ratio-limits: values between these limits are flagged zero.

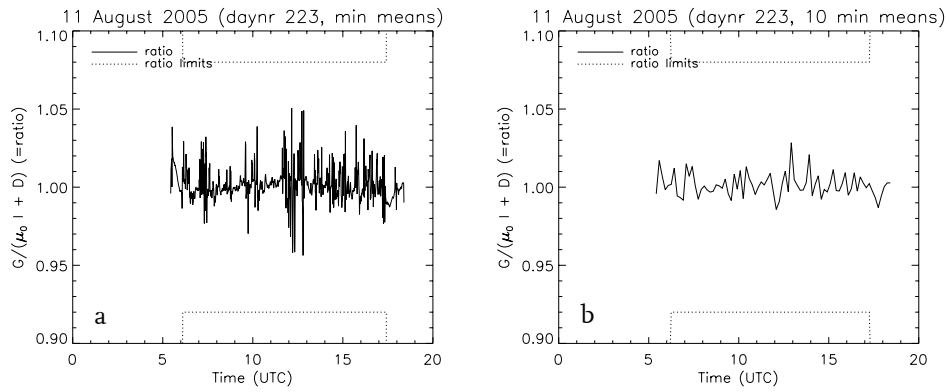


Figure 4.4: The ratio $G/(\mu_0 I + D)$ (a) on the basis of minute means and (b) on the basis of 10 minute means as a function of time (UTC) for 11 August 2005. The dotted lines indicate the ratio-limits: values between these limits are flagged zero.

5. Comparison of pyrhelimetric and pyranometric sunshine duration

5.1 Introduction

In this section, the different methods for the determination of sunshine duration are applied to the solar radiation measurements made in Cabauw and the results are compared.

The sunshine duration for each 10 minute interval is determined from global radiation measurements with the pyranometric methods discussed in chapter 3 (Slob, Bergman and Schipper method) and from DNSI measurements with the pyrhelimetric (or Direct) method. This is done for the period March 2005 - February 2006. From these 10 minute values, daily, monthly or seasonal totals of sunshine duration are determined and the different methods are compared.

The pyrhelimetric sunshine duration, which is the sunshine duration derived from measurements of the direct radiation, is denoted by SD_{Direct} and the pyranometric sunshine duration, which is the sunshine duration derived from global radiation measurements, is denoted by SD_{Slob} , $SD_{Bergman}$ or $SD_{Schipper}$, depending on which variation of the algorithm is used.

First the daily sunshine duration will be discussed. The daily SD_{Direct} during the year is given in Figure 5.1. Also shown in Figure 5.1 is the day-length, which is defined here as the time that the sun is above the horizon ($\mu_o > 0$), so it equals the maximum possible sunshine duration per day. In the next subsection, the daily sunshine duration according to the different pyranometric methods is compared to the daily SD_{Direct} and the sunshine duration during the day is studied. In section 5.3 the monthly and seasonal sunshine duration according to the different methods are investigated. In section 5.4 the sunshine duration as determined by the Bergman method is studied for different solar elevation angles and different cloudiness and it is investigated which parts of the algorithm require improvement. Finally, in section 5.5 the conclusions of comparing

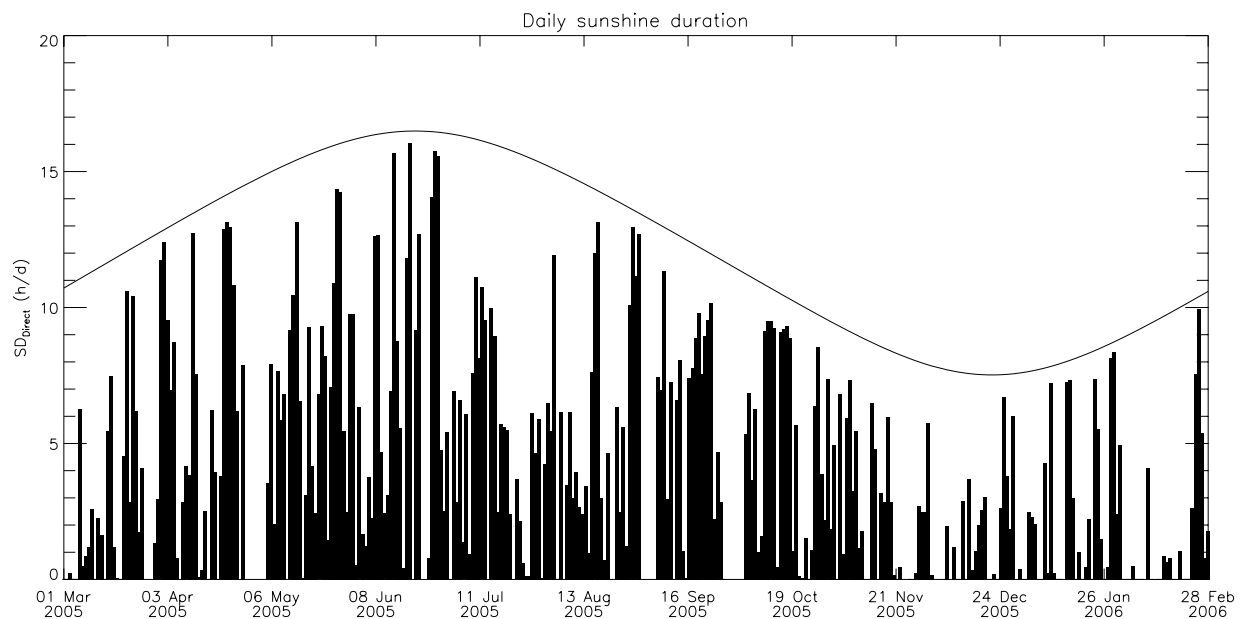


Figure 5.1: Daily sunshine duration (h) according to the Direct method (bars) during the year (March 2005 – February 2006). Also shown is the day-length (solid line), which is defined here as the time of the day when $\mu_o > 0$, and which equals the maximum possible sunshine duration.

the pyranometric and pyr heliometric method are presented, together with suggestions for improvement of the pyranometric method.

5.2 Daily sunshine duration

Figure 5.2a shows the daily pyranometric sunshine duration (h) versus the daily pyr heliometric sunshine duration (h) for the three pyranometric methods (corresponding statistics are listed in Table 5.1). Also shown in Figure 5.2a are the 1:1 line and a fit through the data points. In the ideal case, the fit would coincide with the 1:1 line, because then the results of the pyranometric method would equal those of the pyr heliometric method. The slope and offset of the fit through the data and the spread (standard error in a single observation) of the data around the fit are given in the figure as well.

The left panel in Figure 5.2a clearly shows that, compared to the Direct method, the Slob method underestimates the sunshine duration, which is consistent with the results found by Slob and Monna (1991), while the middle panel in Figure 5.2a shows that the Bergman method overestimates the sunshine duration. The spread in the data is somewhat larger for the Bergman method than for the Slob method, but for the Bergman method the fit seems to be closer to the 1:1 line. The Slob method performs best for days with only few hours of sunshine, while the Bergman method performs better on very sunny days. The sunshine duration as derived by means of the Bergman method is higher than that derived with the Slob method on most days. This overall increase in sunshine duration is caused by the adjustments Bergman made to the original Slob algorithm. The daily sunshine duration is for example increased by also allowing times when $0.05 \leq \mu_0 < 0.1$ to contribute to the sunshine duration. Further also the increase of T_L from 4 to 8, in the part of the algorithm for broken clouds, affects the sunshine duration. When the measured global and estimated diffuse irradiance remain the same, raising T_L increases the fraction of sunshine duration, since it decreases the estimated direct irradiance under cloudless conditions. These adjustments were made by Bergman to find more agreement with the Campbell-Stokes sunshine duration measurements, confirming the idea that the Campbell-Stokes measurements overestimate the sunshine duration (WMO, 1996).

Table 5.1: Yearly totals of sunshine duration for the pyranometric methods (h), also given are the cumulative difference (h/y) and the averaged difference per day (h/d) between each pyranometric method and the pyr heliometric method. ($SD_{Direct} = 1429$ h/year)

	SD_{Slob}	$SD_{Bergman}$	$SD_{Schipper}$
Yearly sunshine duration (h/year)	1357	1620	1546
Cumulative difference ($SD_{Pyranometric} - SD_{Direct}$) (h/year)	-72	191	117
Averaged difference per day ($SD_{Pyranometric} - SD_{Direct}$) (h/d)	-0.22 ± 0.05	0.59 ± 0.04	0.36 ± 0.06

In Figure 5.2b, the differences in daily sunshine duration (h/d) between the pyranometric methods and the pyr heliometric method are shown during the year. This figure again shows that the Slob method mainly underestimates the sunshine duration compared to the Direct method, while the Bergman and Schipper method overestimate the sunshine duration. The averaged difference per day is given in Table 5.1, together with the yearly totals of sunshine duration and the cumulative difference.

The averaged difference per day is largest for the Bergman method, and smallest for the Slob method. Large variations in the differences from day to day can be found for all methods, but particularly for the Schipper method. This suggests that the performance of the pyranometric methods depends on the daily radiation conditions, specifically caused by cloud amount and type. The influence of cloudiness on the performance of a pyranometric method will be investigated in section 5.4.

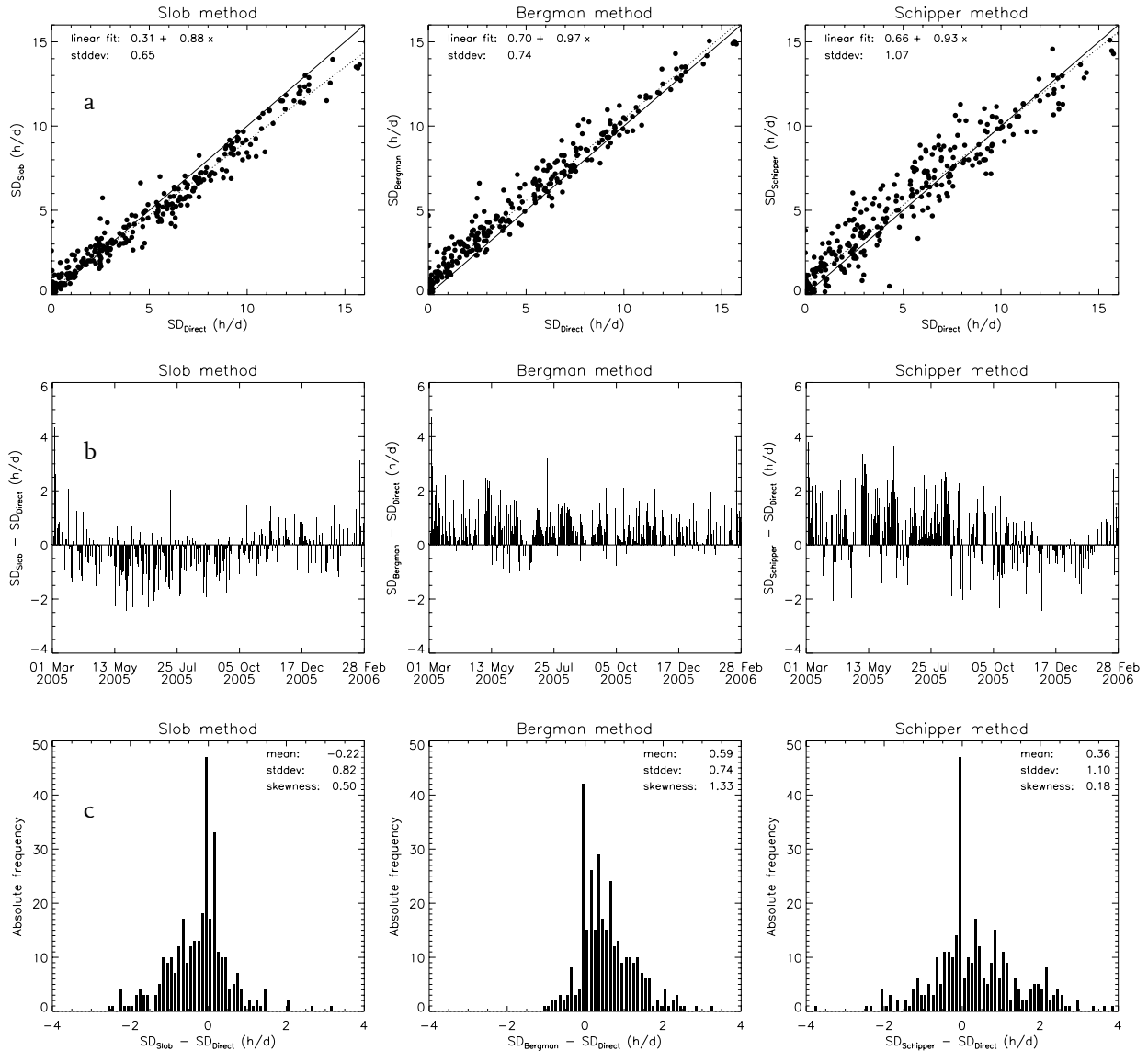


Figure 5.2: (a) Daily sunshine duration (h) according to the Slob method (left panel), the Bergman method (middle panel) and the Schipper method (right panel), against the daily sunshine duration (h) according to the Direct method for March 2005 – February 2006 (points) and a fit through the data (dotted line). The solid line is the 1:1 line, for points on this line the daily sunshine duration derived from the pyranometric method equals that from the pyrheiliometric method. (b) Difference in daily sunshine duration (h) throughout the year: $SD_{Slob} - SD_{Direct}$ (left panel), $SD_{Bergman} - SD_{Direct}$ (middle panel) and $SD_{Schipper} - SD_{Direct}$ (right panel). (c) Absolute frequency of the difference in daily sunshine duration: $SD_{Slob} - SD_{Direct}$ (h/d) (left panel), $SD_{Bergman} - SD_{Direct}$ (h/d) (middle panel) and $SD_{Schipper} - SD_{Direct}$ (h/d) (right panel).

As can be concluded from the right panel in Figure 5.2b, the Schipper method causes the largest scatter compared to the other pyranometric methods, despite the fact that Schipper used a much longer dataset (8 years) than Slob (3 years) and Bergman (< 1 year) to adjust/derive the parameterizations used in the algorithm. For the estimation of the direct irradiance under

cloudless conditions Schipper uses a (much) lower Linke turbidity factor (2.25; 3.24; 4.36) than Bergman (3.5; 6; 10) and Slob (-; 6; 10) use, for all solar elevation angles. This increases the limiting value $(G/G_o)_{gr}$, which is an estimation of the global irradiance under cloudless skies. This means that some periods that are completely sunny according to the Bergman method, are labelled (completely) cloudy by the Schipper method, decreasing the daily sunshine duration compared to $SD_{Bergman}$. For the part of the algorithm that treats periods with broken clouds, Schipper increased the value of the Linke turbidity factor (to 13.03) compared to the Slob (4) and Bergman (8) method. This leads to unrealistic low values of the direct irradiance under cloudless skies, and therefore too high fractions of sunshine duration. On days with broken clouds the daily $SD_{Schipper}$ might thus be higher than $SD_{Bergman}$, while it will be lower than $SD_{Bergman}$ on other days, leading to a large spread in $SD_{Schipper}$ compared to SD_{Direct} . The Schipper method is by no means an improvement compared to the Slob or the Bergman method.

Another way to compare the pyranometric methods with the pyrliometric method is by means of histograms (Figure 5.2c). In the histograms the occurrence of differences in daily sunshine duration between the pyrliometric and pyranometric methods are shown. Since only a year data is available, the histograms are not very smooth, but nonetheless useful to consider. The left panel in Figure 5.2c clearly shows that for the Slob method negative values occur more often than positive values, while the middle panel shows that for the Bergman method most values are positive. The values in the right panel, which shows the differences between the Direct and the Schipper method, seem to be more evenly spread around zero, but the distribution is wider and the averaged difference per day is found to be positive (Table 5.1). Since in this research the real sunshine duration is represented by SD_{Direct} , it can be said that on average the Slob method underestimates the sunshine duration by 0.22 h/d, while the sunshine duration is overestimated by 0.59 h/d by the Bergman method and by 0.36 h/d by the Schipper method. The best agreement is thus found between the Slob method and the pyrliometric method, although all pyranometric methods show a deviation from zero for the average difference in sunshine duration per day.

The standard deviations given in Figure 5.2a are a measure of the scatter of the daily totals of sunshine duration with respect to the linear fit. The standard deviations given in Figure 5.2c on the other hand, are a measure of the spread of the data (difference in daily sunshine duration between the pyranometric and pyrliometric method) around zero. The latter thus presents the accuracy of each pyranometric method with respect to the pyrliometric method. For the Slob method this accuracy is 0.82 h, for the Bergman method 0.74 h and for the Schipper method 1.10 h.

So far, the daily differences in sunshine duration between the pyrliometric and pyranometric methods have been presented in different ways, but nothing has been said about the difference between the methods during the day. In the left panels in Figure 5.3 the sunshine duration during the day is shown, averaged over the whole year, according to the different methods. In the right panels in Figure 5.3 the difference between each pyranometric method and the pyrliometric method is shown, also during the day, averaged over the year. To circumvent the problem of changing day-length throughout the year, the averaging process makes use of the fractional time, where zero represents sunrise and one represents sunset on each day.

In the right panel in Figure 5.3a, dips can be seen at the beginning and the end of the day. These show that on some days the Direct method detects sunshine earlier than the Slob method. Days on which this occurs are mostly summer-days, when the DNSI is already quite strong just after sunrise. When it exceeds 120 Wm^{-2} , the Direct method will see this period as sunny, while

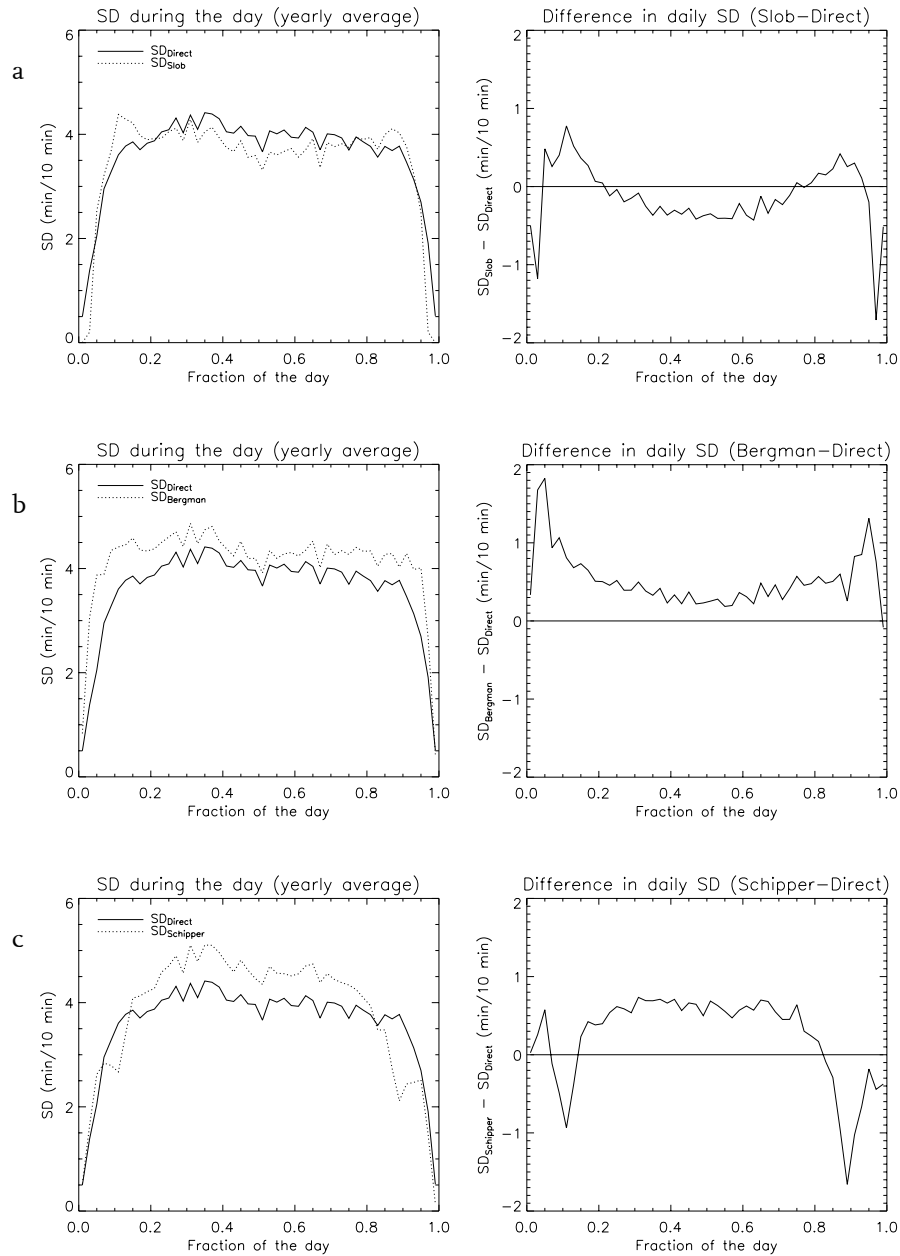


Figure 5.3: Sunshine duration according to each pyranometric method (dotted line) and the pyr heliometric method (solid line) in minutes per 10 minute interval as a function of the day fraction (0=sunrise, 1=sunset), averaged over the period Mar 2005 – Feb 2006 (left panels) and the difference (pyranometric – pyr heliometric) in averaged sunshine duration in minutes per 10 minute interval as a function of the day fraction (right panels) for (a) the Slob method, (b) the Bergman method and (c) the Schipper method.

the sunshine duration according to the Slob method is zero by definition as long as $\mu_0 < 0.1$. Another possible cause of these small dips in Figure 5.3a is the fact that the pyranometric methods use 10 minute mean values of the global radiation to determine the sunshine duration. At low solar elevation angles, a few minutes of sunshine during a 10 minute interval will not make the mean global radiation high enough for the interval to be seen as sunny by the algorithm. The Direct method, however, gives sunshine seconds because the sampling frequency of the pyr heliometer is 1 Hz. However, in Figure 5.3b dips are not observed at the beginning or end of the day. This confirms the idea that the dips in Figure 5.3a are indeed caused by the fact

that the SD_{Slob} is zero for $\mu_o < 0.1$, and that the adjustment of Bergman to lower this to $\mu_o < 0.05$ was enough to solve for this.

Figure 5.3a shows that the Slob method underestimates the sunshine duration at the beginning and end of the day, and also on the middle of the day, while it overestimates the sunshine duration in the morning and late afternoon. The Bergman method overestimates the sunshine duration during the whole day (right panel in Figure 5.3b) and the Schipper method during most of the day, although underestimation of the sunshine duration is found in the morning and from late afternoon until sunset (right panel in Figure 5.3c).

Figure 5.3 shows that the differences between each pyranometric method and the pyr heliometric method vary during the day. This may be caused by different radiation conditions (induced by variations in cloudiness) that occur on particular times during the day, but it can also be caused by the fact that different solar elevation angles are treated differently by the algorithm. For all pyranometric methods, the largest differences with the pyr heliometric method are found at the beginning or end of the day, so for low solar elevation angles.

5.3 Monthly and seasonal sunshine duration

Figure 5.4a shows the monthly sunshine duration according to the three pyranometric methods and the pyr heliometric method and Figure 5.4b shows the seasonal sunshine duration. The seasons are defined meteorologically: spring consist of March, April and May, summer of June, July and August, autumn of September, October and November and winter of December, January and February.

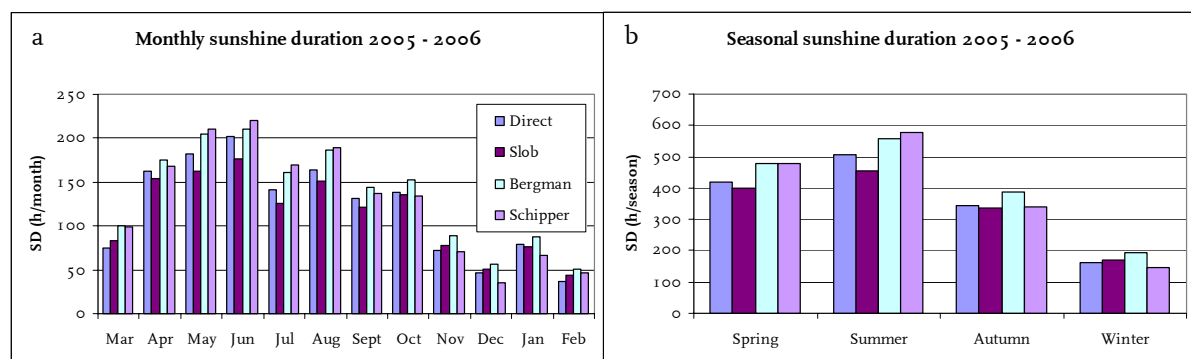


Figure 5.4: (a) Monthly and (b) seasonal totals of sunshine duration (h) according to the Direct, Slob, Bergman and Schipper method.

Figure 5.4a shows that from April to October (and in January) the Slob method underestimates the sunshine duration compared to the Direct method, while it overestimates the sunshine duration during the rest of the year. The Schipper method overestimates the sunshine duration during a large part of the year, but it underestimates the sunshine duration during late autumn and early winter, while the Bergman method overestimates the sunshine duration during the whole year.

Figure 5.4b and Table 5.2 show that the performance of the pyranometric methods compared to the pyr heliometric method is worst in spring and summer. Compared to the Direct method, the Slob and Schipper method perform best in the autumn, while the Bergman method does not seem to perform clearly better in one particular season.

Figure 5.4b shows that the Slob method is actually quite good in representing the sunshine duration on the basis of the WMO threshold and that neither the Bergman nor the Schipper method is a good alternative for this. It was not expected that the Bergman method would perform equally well as the Slob method, since the Bergman method is fitted to the Campbell-Stokes recorder measurements and not to the WMO threshold.

Table 5.2: Differences in sunshine duration (h) between the pyranometric and pyr heliometric methods during the different seasons.

	Spring	Summer	Autumn	Winter	Year
$SD_{\text{Slob}} - SD_{\text{Direct}}$ (h)	-19	-54	-8	9	-72
$SD_{\text{Bergman}} - SD_{\text{Direct}}$ (h)	61	50	44	34	191
$SD_{\text{Schipper}} - SD_{\text{Direct}}$ (h)	58	72	-1	-13	117

Tuning the Bergman method to the Campbell-Stokes measurements causes the SD_{Bergman} to be too high, compared to the Direct method. The Schipper method is expected to perform better than the Bergman method, since it is fitted to the WMO threshold. During autumn and winter the Schipper method does indeed perform better than the Bergman method, but in the summer season it performs worse.

For all pyranometric methods, the difference in sunshine duration with the pyr heliometric method varies throughout the year. Since the maximum value of μ_0 differs per season, the algorithm as used in the pyranometric methods can be used to explain the differences between the seasons. The largest difference within the algorithm can be found between situations for which $\mu_0 < 0.3$ and situations for which $\mu_0 \geq 0.3$, since different parameterizations are used for these μ_0 intervals. In spring and summer, μ_0 reaches its highest values and the criterion $\mu_0 \geq 0.3$ will be met a large part of the day. During part of the winter however, μ_0 does not reach values as high as 0.3 at all. Figure 5.5 shows the behaviour of μ_0 during the year. In Figure 5.5a the maximum value of μ_0 per day during the year is plotted. This figure shows that μ_0 exceeds 0.3 on all days in spring and summer and on most days in autumn too. Figure 5.5b shows the time during which μ_0 exceeds 0.3 each day, in combination with the day-length. This shows that the time during which μ_0 exceeds 0.3 quickly drops to very small values in late autumn and is zero during the first part of the winter. In addition, Figure 5.5c shows the relative time per day that $\mu_0 \geq 0.3$. From Figure 5.5 it can be concluded that the sunshine duration in late autumn and winter is mainly determined by the part of the algorithm for low solar elevation angles. For spring and summer, on the other hand, the part of the algorithm for $\mu_0 \geq 0.3$ is the most important part for the determination of sunshine duration. This also means that, in winter, broken cloud situations

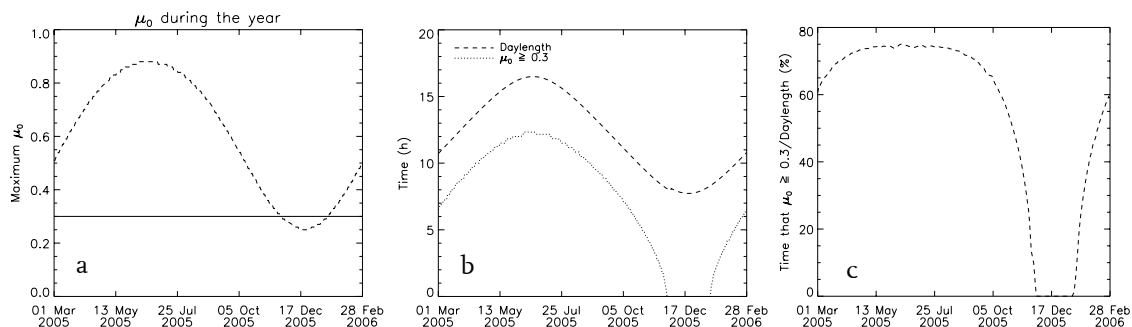


Figure 5.5: (a) The maximum value of μ_0 per day during the year (dashed line) and the line $\mu_0 = 0.3$, (b) the day-length (h) during the year (dashed line) and the time per day (h) that $\mu_0 \geq 0.3$ (dotted line) and (c) the ratio of the time that $\mu_0 \geq 0.3$ and the day-length (in %).

are hardly recognised, and the fraction of sunshine will be either zero or one most of the time, since for $\mu_o < 0.3$ only a fraction of sunshine of 0 or 1 is possible (Figure 3.2).

5.4 Analysis of the Bergman method in terms of solar elevation angle and cloudiness

So far, the Slob, Bergman and Schipper method have been discussed in comparison to the Direct method, but from now on the focus will be on the Bergman method. This method will be discussed in more detail, because this method is operationally used by the Klimatologische Dienst (Climatological Service) at the KNMI to determine the sunshine duration on 32 stations in the Netherlands.

The daily, monthly and seasonal totals of sunshine duration according to the Bergman and Direct method have been discussed and intercompared. In these considerations, all available data was used and no distinction between different solar elevation angles or cloud amount was made. However, the algorithm, which is used in the Bergman method to determine the sunshine duration, distinguishes between different solar elevation angle intervals (section 3). This means that the Bergman method might perform different for different solar elevations. Further, the amount and type of clouds will affect the sunshine duration, but it is not known how well this effect is captured by the Bergman method and whether the Bergman method performs better under certain cloudiness conditions.

In this section, the effect of different solar elevation angles and cloudiness conditions on the performance of the Bergman method will be studied in comparison with the Direct method.

5.4.1 Solar elevation angle

In Figure 5.6, histograms of the differences in daily sunshine duration between the Bergman and the Direct method are shown for each μ_o interval that the algorithm distinguishes. The criteria for the different μ_o intervals are based on the Bergman algorithm: (a) $\mu_o < 0.05$, (b) $0.05 \leq \mu_o \leq 0.087$, (c) $0.087 < \mu_o < 0.3$ and (d) $\mu_o \geq 0.3$. By using this separation, the results may give insight in the performance of the different parts of the algorithm.

Figure 5.6a gives the histogram for the times the sun is just above the horizon: $\mu_o < 0.05$. For these solar elevation angles, the sunshine duration according to the Bergman method is zero by definition. It is interesting though, to examine this assumption that is made in the algorithm. If the sunshine duration according to the Direct method is much larger than zero, it might be relevant to adjust the algorithm at this point. In Table 5.3, the total sunshine duration according to both methods is given for each μ_o interval. Table 5.3 also gives the averaged difference per day, and this turns out to be less than 0.02 h for very low elevation angles, so it seems that the algorithm does not need to be adjusted for $\mu_o < 0.05$.

For $0.05 \leq \mu_o \leq 0.087$ (Figure 5.6b) the differences are a little larger, but still the algorithm seems to perform quite good on average. Table 5.3 shows that the largest differences can be found for $0.087 < \mu_o < 0.3$ (Figure 5.6c) and $\mu_o \geq 0.3$ (Figure 5.6d). This is understandable, because the solar elevation angles that are associated with these μ_o occur during a large part of the day, so most of the sunshine duration during a day will be during these solar angles.

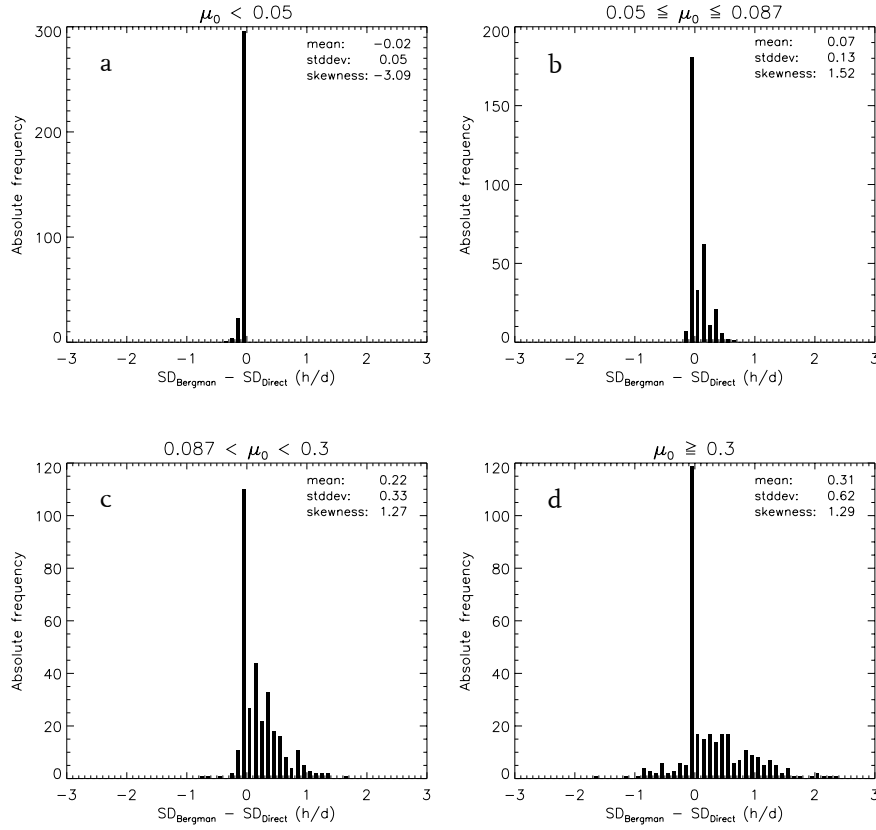


Figure 5.6: Histograms of $SD_{Bergman} - SD_{Direct}$ (h/d) for (a) $\mu_0 < 0.05$, (b) $0.05 \leq \mu_0 \leq 0.087$, (c) $0.087 < \mu_0 < 0.3$ and (d) $\mu_0 \geq 0.3$.

Figure 5.3b showed that the Bergman method overestimates the sunshine duration compared to the Direct method throughout practically the whole day, which is confirmed by Table 5.3 and Figure 5.6. Figure 5.3b further showed that the largest difference between $SD_{Bergman}$ and SD_{Direct} is found for small μ_0 , at the beginning and end of the day. At first sight this seems in disagreement with Table 5.3, which shows that the largest differences can be found for larger μ_0 , but this is caused by the fact that $\mu_0 \geq 0.3$ occurs during quite a long portion of the day, at least in spring and summer (Figure 5.5). So although the differences in sunshine duration between the Direct and the Bergman method at the beginning and end of the day are larger than during most of the day, the yearly total of $SD_{Bergman} - SD_{Direct}$ is largest for higher solar elevation angles. Improvement of the algorithm for $\mu_0 < 0.3$ will thus, on average, increase the agreement between the Bergman and Direct method during the day, but improvement of the part of the algorithm for $\mu_0 \geq 0.3$ might be necessary to increase the agreement in totals of sunshine duration between the Bergman and Direct method.

Table 5.3: Yearly totals of $SD_{Bergman}$ (h) and SD_{Direct} (h) for different μ_0 intervals, and the averaged difference in sunshine duration between the Bergman and the Direct method (h/d).

μ_0 interval	All μ_0	$\mu_0 < 0.05$	$0.05 \leq \mu_0 \leq 0.087$	$0.087 < \mu_0 < 0.3$	$\mu_0 \geq 0.3$
$SD_{Bergman}$ (h/year)	1620	0	54	431	1135
SD_{Direct} (h/year)	1429	6	29	358	1037
$SD_{Bergman} - SD_{Direct}$ averaged per day (h/d)	0.59 ± 0.04	-0.018 ± 0.003	0.075 ± 0.007	0.224 ± 0.018	0.305 ± 0.034

5.4.2 Cloudiness

Besides a separation into μ_o intervals, it is also possible to separate the data into completely sunny, completely cloudy and partly cloudy conditions. The criteria to separate the data into these different weather situations are again based on the Bergman algorithm. A period is now said to be completely sunny if it is completely sunny according to the algorithm (fraction sunshine = 1), which means that it does not have to be completely sunny according to the Direct method. Then SD_{Bergman} is compared to SD_{Direct} for the same period. Measurements for which $\mu_o < 0.05$ are omitted for this analysis since the SD_{Bergman} is zero by definition for these μ_o and no further division into sunny or cloudy is thus possible. For the intervals $0.05 \leq \mu_o \leq 0.087$ and $0.087 < \mu_o < 0.3$ the algorithm distinguishes only between completely sunny and completely cloudy periods, while for $\mu_o \geq 0.3$ also partly cloudy situations can be recognised. Figure 5.7 shows the histograms for the daily differences between SD_{Bergman} and SD_{Direct} for sunny, cloudy and partly cloudy conditions. For each situation, the yearly total sunshine duration according to the two methods is given in Table 5.4, together with the averaged difference per day.

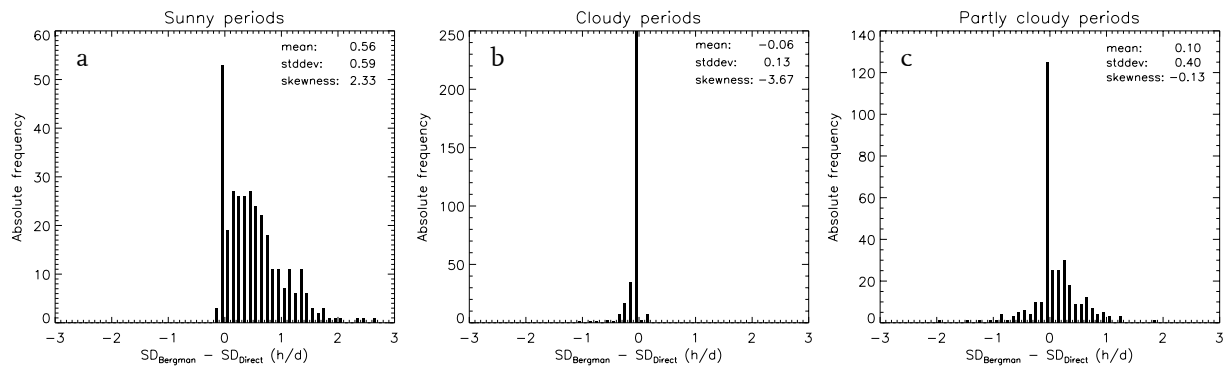


Figure 5.7: Histograms of $SD_{\text{Bergman}} - SD_{\text{Direct}}$ (h/d) for (a) sunny periods, (b) cloudy periods and (c) partly cloudy periods (according to the algorithm).

According to Figure 5.7b, periods that are completely cloudy according to the Bergman method are also (almost) completely cloudy according to the Direct method, the averaged difference between the methods being only -0.06 hours per day (Table 5.4).²

Table 5.4: Yearly totals of SD_{Bergman} (h) and SD_{Direct} (h) for completely sunny, completely cloudy and partly cloudy periods (according to the algorithm) and the averaged difference in sunshine duration between the Bergman and the Direct method (h/d).

	Sunny periods	Cloudy periods	Partly cloudy periods
SD_{Bergman} (h/year)	1335	2	282
SD_{Direct} (h/year)	1155	20	248
$SD_{\text{Bergman}} - SD_{\text{Direct}}$ averaged per day (h/d)	0.56 ± 0.03	-0.06 ± 0.01	0.10 ± 0.02

² The fact that the yearly total of SD_{Bergman} is not zero for the cloudy periods is caused by the rounding off of the numbers that are used to create the histograms (to create the histograms a μ_o with only two significant numbers is used, while a higher accuracy is used in the algorithm itself). This problem only occurs a few times, still leaving the sum of sunshine duration by the Bergman method close to zero, so that the general conclusions are not affected by this small problem.

Under sunny conditions (Figure 5.7a) the differences between the algorithm and the Direct method are much larger than for the cloudy periods. On average this difference is about 0.56 h/d. For the partly cloudy periods (Figure 5.7c) $SD_{\text{Bergman}} - SD_{\text{Direct}}$ is about 0.10 h/d on average.

From these histograms it can thus be concluded that periods that are cloudy according to the algorithm are also cloudy according to the Direct method. Periods that are (completely) sunny according to the algorithm are found to be less sunny according to the Direct method, however.

For the smaller μ_o this can be understood, because at these angles only a fraction of sunshine of zero or one is possible, and nothing in between. So periods that are partly sunny might be counted as sunny, thereby overestimating the real sunshine duration. The algorithm might be improved at this point by also permitting fractions between zero and one. Another way of improving the algorithm could be by adjusting the limiting value. This could be done in such a manner that 10 minute intervals that are mostly sunny are counted as completely sunny, while intervals during which the sun shone only a short time are counted as completely cloudy. The sunshine duration will then be overestimated in some intervals and underestimated in others, which might improve the algorithm on daily totals of sunshine duration. For the larger μ_o the algorithm is more complicated, and a specific cause for the overestimation of sunshine duration by the algorithm cannot be given without further examination. The limiting value $(G/G_o)_{gr}$ (estimation of the global radiation under cloudless conditions; section 3.2) also plays an important role in this part of the algorithm though, so possibly adjustment of this value might improve this part of the algorithm.

To study the differences between the Bergman and the Direct method in more detail, the sunshine duration on individual days is examined. These individual days will be discussed according to the cloudiness on a day. A classification into different cloud types is made by visual inspection of the daily courses of global, diffuse and direct normal solar irradiance.

The cloud types that are distinguished are: completely cloudless, completely cloudy, broken clouds and cirrus. In the case of broken clouds solar radiation is blocked by a cloud now and then. This means that the DNSI will jump from zero (cloud in front of the sun) to its maximum value on this particular day (no cloud in front of the sun). With cirrus high, optically thin ice clouds are meant. Contrails also belong to this type. These high clouds are often thin enough for the sun to be visible, but they do reduce the intensity of the solar radiation. In the case of cirrus, the DNSI will be less than its maximum value, but will normally not become zero.

For the classification into different cloud types, also cloud images of the Total Sky Imager are used (Cloudnet database). The Total Sky Imager consists of a hemispherical mirror facing the sky, and a camera that looks down on this mirror, to make images of the sky. The system also involves a sun-blocking shadowband to block the intense direct radiation from the sun. During day time the Total Sky Imager at Cabauw takes an image of the sky every 10 minutes. These sky images are then analysed for fractional cloud cover. Figure 5.8 shows some examples of total sky images during (a) a cloudless day, (b) a cloudy day, (c) a day with broken clouds and (d) a day with cirrus. Beneath each image the time (UTC) and fractional cloud cover of respectively thin and opaque clouds are given.

For each examined day, the direct normal, global and diffuse solar irradiance are plotted as a function of time during the day. Further, the sunshine duration during the day according to the Direct and Bergman method and the difference ($SD_{\text{Bergman}} - SD_{\text{Direct}}$) are plotted, in minutes per 10 minute interval.

Some examples of individual days will be discussed here, which have been selected according to the dominating clouds on that particular day. On most days, however, not just one particular

cloud type dominates, but a combination of different types can be seen during the day. These days have also been studied, and the results as given below are also valid for fractions of days on which this cloud type dominates.

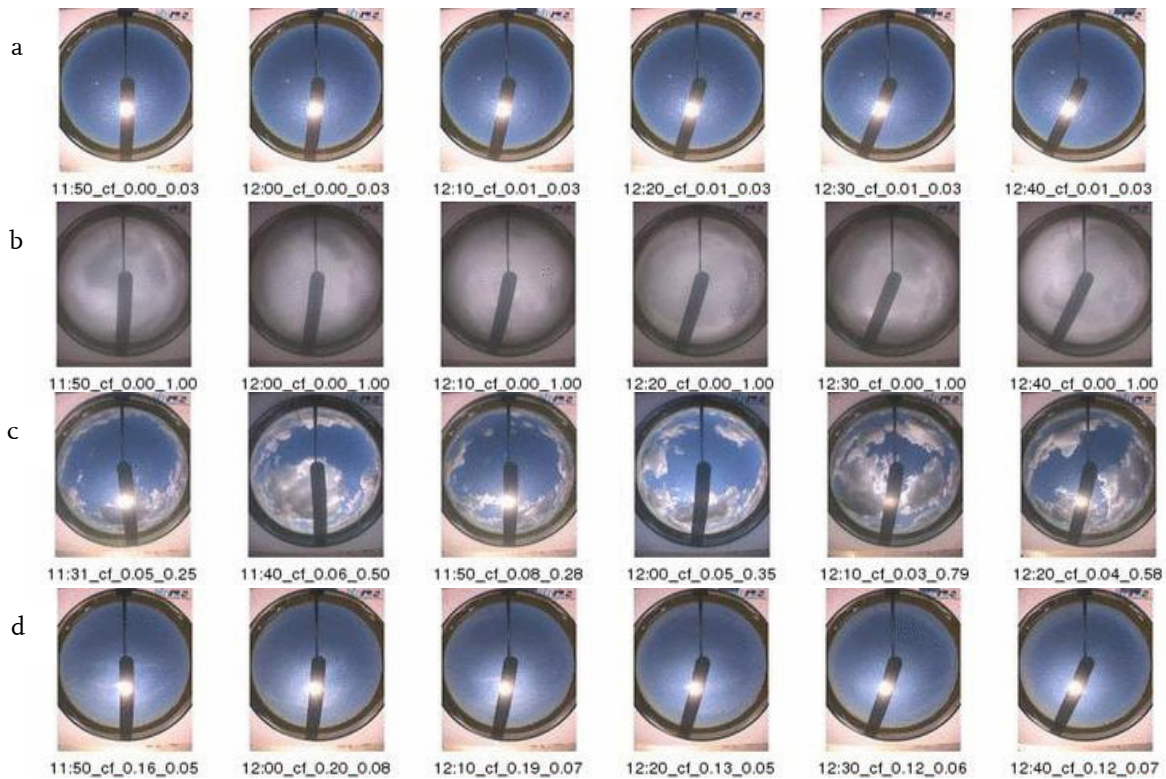


Figure 5.8: Images of the Total Sky Imager for (a) a cloudless day (June 19th 2005), (b) a cloudy day (June 2nd 2005), (c) a day with broken clouds (April 27th 2005) and (d) a day with cirrus (June 27th 2005).

Cloudless

First the cloudless days are treated. An example of a cloudless day is June 19th 2005. Figure 5.9a shows the different radiation components on this day. It can be seen that the direct irradiance is very high and the variation with time is rather smooth. The diffuse irradiance is relatively low, indicating that this was indeed a cloudless day. The differences between the two methods are quite small on this day, only at the beginning and end of the day the Bergman method underestimates the sunshine duration a little, a pattern that is also found for other sunny days.

In general the Bergman method gives a good estimate of the sunshine duration for cloudless periods. The only differences between the two methods on cloudless days occur at the beginning

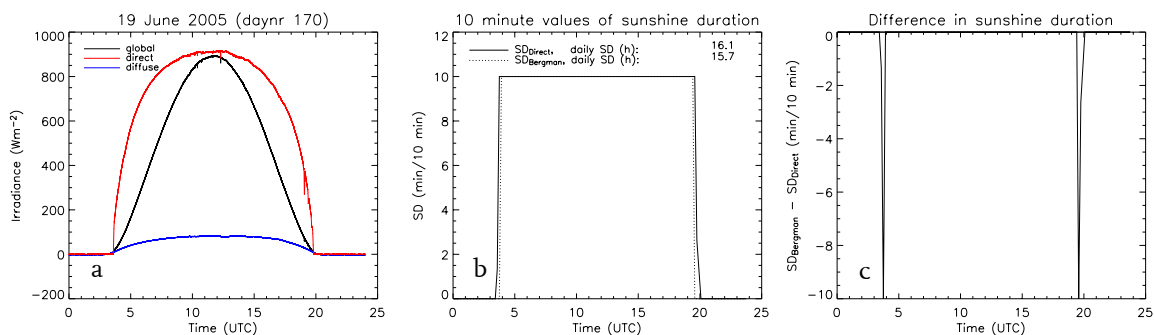


Figure 5.9: (a) Direct normal, global and diffuse solar irradiance (in Wm^{-2}) (b) sunshine duration during the day according to both methods and (c) difference in sunshine duration between the two methods as a function of time (UTC), on 19 June 2005. Difference in daily $SD_{Bergman} - SD_{Direct} = -0.40$ h.

and end of the day. At these moments the Bergman method slightly underestimates the sunshine duration. This underestimation might be due to the fact that according to the Bergman method the sunshine duration is zero for $\mu_0 < 0.05$ by definition, while there can be sunshine duration according to the Direct method. This effect is thought to play a role mainly in summer, when the threshold of 120 Wm^{-2} is exceeded just after sunrise. Further also the averaging of the global radiation over 10 minutes for the Bergman method might affect the sunshine duration just after sunrise and just before sunset. The 10 minute average of the global radiation might then be too low, so that the Bergman method detects the whole period as cloudy, even when there were some sunshine minutes.

The underestimation of sunshine duration by the Bergman method compared to the Direct method is of the order of 10 minutes for a cloudless beginning or ending of the day.

Cloudy

Figure 5.10 shows the radiation components, the sunshine duration and difference in sunshine duration for June 2nd, which is an example of a cloudy day. Figure 5.10a shows that there is only little direct radiation at the end of the day and that the diffuse radiation is quite high during the whole day; indicators of a cloudy day.

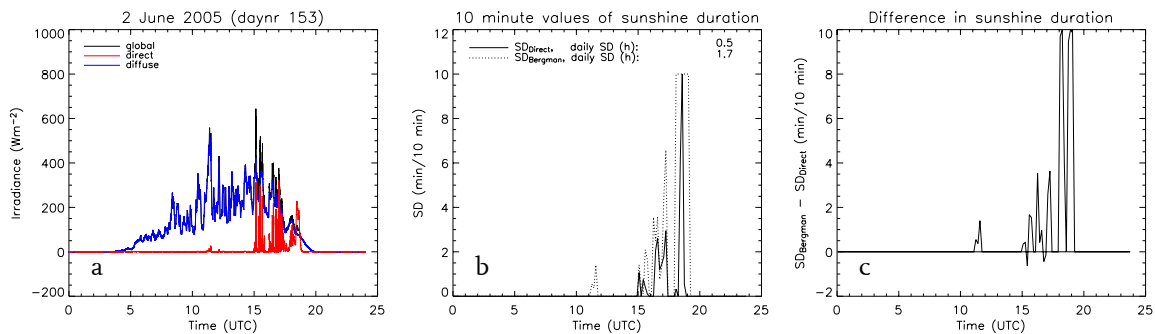


Figure 5.10: (a) Direct normal, global and diffuse solar irradiance (in Wm^{-2}) (b) sunshine duration during the day according to both methods and (c) difference in sunshine duration between the two methods as a function of time (UTC), on 2 June 2005. Difference in daily $SD_{\text{Bergman}} - SD_{\text{Direct}} = 1.15 \text{ h}$.

During most of the day the sunshine duration is zero, according to both methods, while it is larger than zero in the presence of direct radiation. The Bergman method overestimates the sunshine duration on the middle of the day, when some direct irradiance comes through the clouds. At the end of the day, more radiation can reach the ground and both methods determine some sunshine, but again the Bergman method gives an overestimation.

Figure 5.11 shows the results for March 2nd 2005, a completely cloudy day. The estimation of the sunshine duration by the Bergman method is in good agreement with the SD_{Direct} on this day. On cloudy days, the estimation of the sunshine duration by the Bergman method is in general in good agreement with the sunshine duration as determined by the Direct method. The only exception to this is when there is also some direct irradiance present, on which the Bergman method instantly reacts. In the presence of direct irradiance the global irradiance will increase. Due to extra reflection at clouds, the diffuse irradiance also increases, thereby increasing the global irradiance even more. As long as the direct irradiance does not exceed the threshold of 120 Wm^{-2} , the Direct method will not determine any sunshine. The increase in global irradiance seems to be enough however, for the Bergman method to estimate a sunshine duration larger than zero, despite the use of 10 minute means of the global radiation.

The overestimation of the Bergman method, compared to the Direct method, is of the order of 10 minutes for a cloudy beginning or ending of the day, and can be about half an hour to an hour a day when direct irradiance is present in combination with clouds during the day.

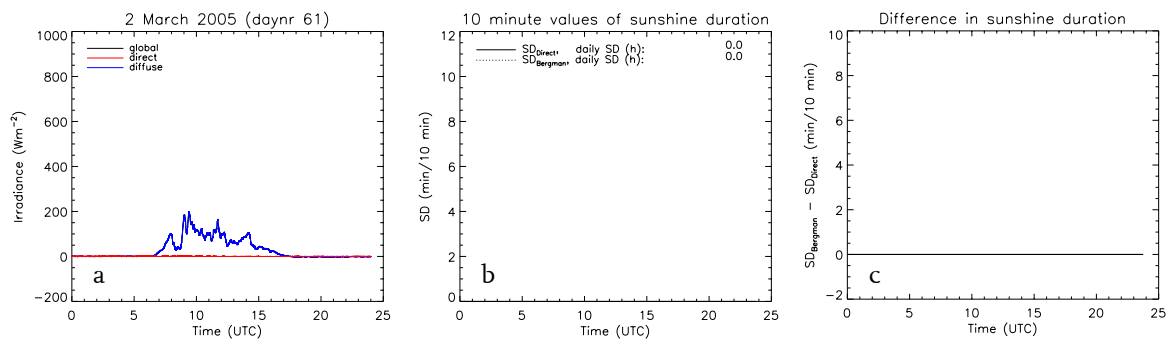


Figure 5.11: (a) Direct normal, global and diffuse solar irradiance (in Wm^{-2}) (b) sunshine duration during the day according to both methods (all values are zero) and (c) difference in sunshine duration between the two methods as a function of time (UTC), on 2 March 2005. Difference in daily $SD_{Bergman} - SD_{Direct} = 0.0$ h.

Broken clouds

A day on which broken clouds were present during most of the day is for example April 27th 2005. For this day, the radiation components, sunshine duration according to both methods and the difference in sunshine duration between the methods are given in Figure 5.12. The DNSI, as shown in Figure 5.12a, jumps from very high values during sunny periods to zero when a cloud obscures the sun. The diffuse irradiance is higher than on completely sunny days, due to reflection at clouds. The difference in sunshine duration between the two methods is positive during most of the sunny periods. Only at the beginning of the day, when it is cloudy, and at the end of the afternoon when it is completely sunny, the difference is zero. During most of the day the Bergman method thus overestimates the sunshine duration.

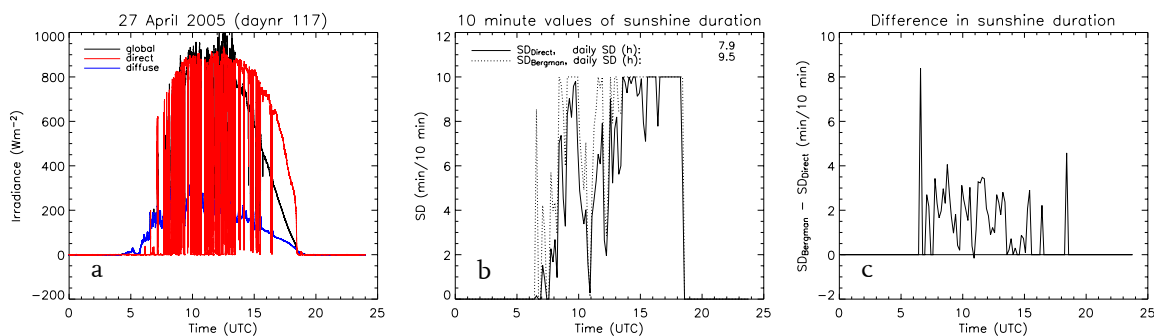


Figure 5.12: (a) Direct normal, global and diffuse solar irradiance (in Wm^{-2}) (b) sunshine duration during the day according to both methods and (c) difference in sunshine duration between the two methods as a function of time (UTC), on 27 April 2005. Difference in daily $SD_{Bergman} - SD_{Direct} = 1.67$ h.

From studying days with broken clouds, it can be concluded that compared to the Direct method, the Bergman method in general overestimates the sunshine duration during periods with broken clouds.

At low solar elevation angles ($\mu_0 < 0.3$) this overestimation is probably caused by the fact that the Bergman method uses 10 minute mean values of the global irradiance. The strong fluctuations of the direct irradiance, that are a feature of broken cloud situations, do not appear so strongly in these averages. The 10 minute means of the global irradiance can remain quite high

during broken clouds if a substantial part of the interval was indeed sunny. For these μ_0 the algorithm only distinguishes between completely sunny and completely cloudy. This means that if the global irradiance is high enough (due to reflection of solar radiation at cloud sides), the whole period will be labelled sunny, even though some minutes might have been cloudy. The overestimation of the sunshine duration by the Bergman method suggests that this occurs more often than the reverse: that the period is mostly cloudy and the whole period is thus labelled cloudy. This result was also seen in the histograms (Figure 5.7), which showed that periods which the algorithm considers as cloudy are also cloudy according to the Direct method, but that periods which are (completely) sunny according to the algorithm are less sunny according to the Direct method.

For the larger solar elevation angles ($\mu_0 \geq 0.3$) the broken cloud situations will be recognised if the difference between the minimum and maximum of the global irradiance in a 10 minute interval is large enough. This situation is treated in the last part of the algorithm (section 3.2.1), where the fraction of sunshine is estimated by subtracting an estimated value for the diffuse irradiance from the measured 10 minute mean of the global irradiance, and then dividing this by an estimation of the direct irradiance under cloudless skies. Slob pointed out that he chose the relatively low value of $T_L = 4$ in this last part of the algorithm, to compensate for the fact that all periods with direct irradiance contribute to the sunshine duration. Bergman increased the Linke turbidity factor from 4 to 8. This decreases the estimated value of the direct irradiance under clear skies and thereby increases the fraction of sunshine, when the global irradiance is kept the same. Apparently the direct irradiance under clear skies is now underestimated, leading to an overestimation of the sunshine duration for broken cloud conditions. A lowering of the Linke turbidity factor in this part of the algorithm might thus decrease the difference between the two methods at this point.

The overestimation of the Bergman method compared to the Direct method is of the order of one or two hours for a day on which broken clouds dominate.

Cirrus

The last cloud-type to be discussed is cirrus. A clear example of a day on which cirrus appeared is June 27th 2005 (Figure 5.13). Especially in the morning and late afternoon, quite a lot of cirrus was present, which is reflected in the variations in the DNSI, which are much larger than on a cloudless day (cf. Figure 5.9a), but smaller than in the case of broken clouds (cf. Figure 5.12a).

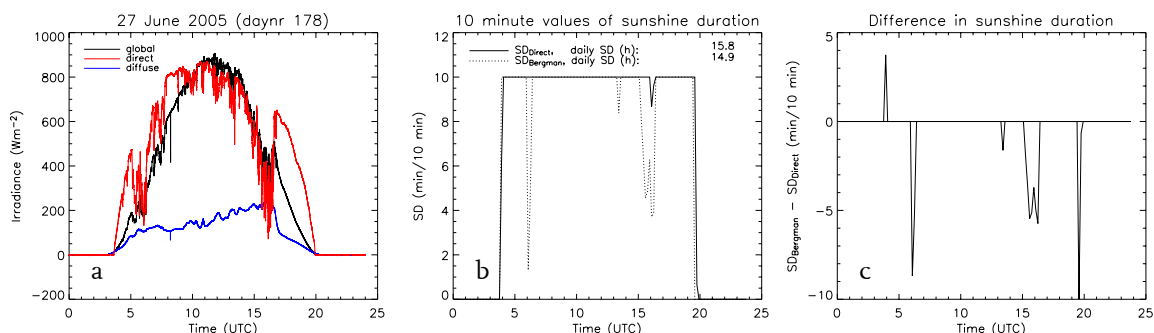


Figure 5.13: (a) Direct normal, global and diffuse solar irradiance (in Wm^{-2}) (b) sunshine duration during the day according to both methods and (c) difference in sunshine duration between the two methods as a function of time (UTC), on 27 June 2005. Difference in daily $SD_{Bergman} - SD_{Direct} = -0.88$ h.

The Bergman method underestimates the sunshine duration during times when a lot of cirrus is present, as can be seen by comparing Figure 5.13a with Figure 5.13c. The end of the day is

completely sunny again, which leads to an underestimation of the sunshine duration by the Bergman method. At the beginning of the day some (high) clouds seem to be present at the horizon. In combination with small μ_o , the increase in diffuse (and thus global) irradiance may be large enough for the Bergman method to estimate sunshine, thereby overestimating the sunshine duration.

For cirrus, two main cases can be distinguished. When only little cirrus is present, the Bergman algorithm performs well and the difference between the two methods is zero, as on a cloudless day. When a lot of cirrus is present however, the direct irradiance is decreased to a larger extent, but often remains above 120 Wm^{-2} , so that the Direct method labels the period as sunny. In these cases, the fraction of sunshine as estimated by the Bergman method is often less than 1, meaning that the Bergman method underestimates the sunshine duration compared to the Direct method.

The underestimation in the presence of dense cirrus-fields shows that the algorithm cannot distinguish cirrus from other clouds very well. Although the sun is visible through the clouds (almost) all the time, the algorithm estimates that there are some periods during which the fraction of sunshine duration is smaller than 1. The variations in the direct irradiance might be so large in these cases that the difference between the minimum and maximum of the global irradiance in a 10 minute interval exceeds the limit for clear skies, indicating that there were clouds during the interval. These cases are then treated in the part of the algorithm for broken clouds, giving values for the fraction of sunshine between 0 and 1. For the broken cloud situations this part of the algorithm caused an overestimation of the sunshine duration by the Bergman method, but for cirrus situations the opposite is the case. The diffuse irradiance is now much lower than in the case of broken clouds, but it is estimated by the same parameterization, giving too high values for cirrus skies and thereby underestimating the direct irradiance and consequently the sunshine duration.

The underestimation of sunshine duration by the Bergman method compared to the Direct method is of the order of half an hour on days where optically thick cirrus is present.

5.5 Conclusions and suggestions for improvement

The Bergman algorithm distinguishes four μ_o intervals: (1) $\mu_o < 0.05$, (2) $0.05 \leq \mu_o \leq 0.087$, (3) $0.087 < \mu_o < 0.3$ and (4) $\mu_o \geq 0.3$. For $\mu_o < 0.05$ the sunshine duration according to the pyrheliometric method is very small, which is correctly represented in the algorithm. Values for μ_o in the second interval only occur during a short time of the day. This means that it will be difficult to derive parameterizations for this μ_o interval, since only few measurements are available. No clear reason is given by Bergman or found here why this interval is treated separately, which is why it will be combined with the third interval to form one interval for the lower solar elevation angles. Examination of the sunshine duration during the day, averaged over the year, show that the largest differences in sunshine duration between the Bergman and the Direct method are found for these μ_o , suggesting that improvement of this part of the algorithm is desired. On the other hand, averaged over the year, the largest daily differences between SD_{Bergman} and SD_{Direct} are found for $\mu_o \geq 0.3$. Despite smaller differences in sunshine duration for $\mu_o \geq 0.3$ during the day, this last μ_o interval is of great importance for the sunshine determination, since $\mu_o \geq 0.3$ occurs during a long portion of the day, at least in spring and summer. Improvement of the algorithm for $\mu_o < 0.3$ will thus, on average, increase the agreement between the Bergman and

Direct method during the day, but improvement of the part of the algorithm for $\mu_o \geq 0.3$ might be more effective to increase the agreement in totals of sunshine duration between the Bergman and Direct method.

Examination of individual days showed that the Bergman algorithm performs quite well under completely cloudy and completely sunny skies during the day. As soon as a cloud blocks the direct solar irradiance however, or some direct solar irradiance comes through the clouds, the estimation of the sunshine duration by the Bergman algorithm is in less agreement with the sunshine duration determined by the Direct method. This indicates that the part of the algorithm treating partly cloudy situations needs reconsidering. Furthermore, for the lower solar elevation angles it is desirable to also allow partly cloudy periods. Currently only completely sunny or completely cloudy periods are distinguished for these μ_o , but the Bergman method is found to overestimate the sunshine duration during (partly) sunny periods. Besides, it seems realistic to also allow partly sunny periods for this part of the algorithm, since broken cloud situations can also occur when $\mu_o < 0.3$. When a lot of cirrus is present, the Bergman method underestimates the sunshine duration, but more often only optically thin cirrus is present, which does not affect the sunshine duration as determined by either the Direct or the Bergman method. The possibility to distinguish cirrus from other clouds is therefore of less importance.

Suggestions for improvement of the pyranometric method are thus:

1. Combine the μ_o intervals $0.05 \leq \mu_o \leq 0.087$ and $0.087 < \mu_o < 0.3$.
2. Also allow partly cloudy periods for the μ_o interval $0.05 \leq \mu_o < 0.3$.
3. Reconsider the part of the algorithm that treats partly cloudy periods, probably the value for T_L is too high for this part.
4. Improvement of the algorithm for the lower as well as the higher solar elevation angles is desired, possibly the two μ_o intervals $0.05 \leq \mu_o < 0.3$ and $\mu_o \geq 0.3$ can be optimized separately, after which the results can be combined to obtain the best algorithm.

In the next chapter, these suggestions for improvement will be used to construct an improved version of the Bergman algorithm. The parameterizations used in this improved algorithm will be derived from solar radiation measurements and the agreement with the parameterizations in the Bergman algorithm will be examined. The effect of different adjustments to the algorithm will then be studied by means of a sensitivity analysis in which the sunshine duration is determined with different adjusted algorithms.

6. Improvement of the pyranometric method

The sunshine duration as determined with the Slob, Bergman and Schipper method has now been compared to the sunshine duration as determined with the Direct method in different ways. The results showed that there are differences between the methods, which vary throughout the year. In this chapter improvement of the Bergman algorithm is investigated by applying the suggestions for improvement summarized in section 5.5. In section 6.1 the basic adjustments to the Bergman algorithm are described, but most parameterizations are left unchanged. In section 6.2 the parameterizations that are used in the Bergman algorithm are compared to solar radiation measurements. For this study, 10 minute means of the global, diffuse and direct normal irradiance are used. In section 6.3 new parameterizations, as derived from the measurements in section 6.2, are implemented into the algorithm constructed in section 6.1 and the effect of different adjustments to the algorithm on the sunshine duration is examined. The sunshine duration determined with these adjusted algorithms is then compared to the sunshine duration according to the Bergman and Direct method. Furthermore, the sunshine duration from the adjusted algorithm that is in best agreement with the Direct method is discussed in more detail. Finally, in section 6.4, a completely different form of the algorithm is studied, in which the sunshine duration is linearly related to the global radiation. The sunshine duration determined with this algorithm is also compared to that of the Bergman algorithm and to that of the best adjusted algorithm found in section 6.3.

6.1 Adjusting the algorithm

In the Bergman algorithm, parameterizations are used to estimate the direct and diffuse radiation components. For the different μ_o -intervals different parameterizations are possible. Before trying to improve the Bergman method, first the Bergman algorithm itself is repeated here:

$$\begin{aligned} \mu_o I / G_o &= \exp(-T_L / (0.9 + 9.4\mu_o)) && (= \text{estimation of direct irradiance under clear skies}) \\ (G/G_o)_{gr} &= D/G_o + \mu_o I / G_o && (= \text{estimation of global irradiance under clear skies;} \\ &&& \text{limiting value}) \end{aligned}$$

If $\mu_o < 0.05$: then fr = 0

If $0.05 \leq \mu_o \leq 0.087$:

$$\begin{aligned} T_L &= 3.5 \\ D/G_o &= 0.2 + \mu_o/3 \\ \text{if}(G/G_o < (G/G_o)_{gr}) &&& \text{then fr} = 0 \quad \text{else fr} = 1 \end{aligned}$$

If $0.087 < \mu_o < 0.3$:

$$\begin{aligned} T_L &= 6 \\ D/G_o &= 0.2 + \mu_o/3 \\ \text{if}(G/G_o < (G/G_o)_{gr}) &&& \text{then fr} = 0 \quad \text{else fr} = 1 \end{aligned}$$

If $\mu_o \geq 0.3$:

$$\begin{aligned} T_L &= 10 \\ D/G_o &= 0.3 \\ \text{if}(G_{max}/G_o < 0.4) &&& \text{then fr} = 0 \quad \text{else} \\ \text{if}(G_{min}/G_o > (G/G_o)_{gr}) &&& \text{then fr} = 1 \quad \text{else} \end{aligned}$$

if($G_{\max}/G_o > (G/G_o)_{gr}$ and $(G_{\max}/G_o - G_{\min}/G_o) < 0.1$) then fr = 1 else
 $T_L = 8$
 $D/G_o = 1.2G_{\min}/G_o$
 if($D/G_o > 0.4$) then $D/G_o = 0.4$ then fr = $(G/G_o - D/G_o) / (\mu_o I/G_o)$

This algorithm will serve as the reference, and thus the Bergman method as the reference pyranometric method for the determination of sunshine duration, since this is the method that is operationally used for the determination of sunshine duration within the KNMI network of meteorological stations in the Netherlands.

The first two suggestions done in section 5.5 for improvement of the pyranometric method can now be applied directly to the algorithm. This means that the μ_o intervals $0.05 \leq \mu_o \leq 0.087$ and $0.087 < \mu_o < 0.3$ are combined and that the part of the algorithm for partly cloudy periods is used for all μ_o . The separation at $\mu_o = 0.3$ is maintained for the moment, although the effect of no separation will also be studied. Suggestions 3. and 4. from section 5.5 need additional investigation to obtain concrete adjustments that can be implemented into the algorithm. These adjustments will be further studied in section 6.2 and 6.3.

In the Bergman algorithm, the diffuse irradiance is limited for broken cloud situations, to prevent the occurrence of very high values that could cause the sunshine duration to be zero when some direct irradiance might still be present. In reality, however, the diffuse irradiance can sometimes obtain values larger than this limit, which will therefore also be allowed in the adjusted algorithm. If the estimates of the diffuse and direct irradiance that are used in the algorithm are realistic, the estimates of the sunshine duration are thought to be realistic too, whether the diffuse irradiance is larger than some limit or not.

Taking into account these considerations, the basic form of the adjusted algorithm becomes:

$$\mu_o I/G_o = \exp(-T_L / (0.9 + 9.4\mu_o))$$

$$(G/G_o)_{gr} = D/G_o + \mu_o I/G_o$$

If $\mu_o < 0.05$ then fr = 0
 If $0.05 \leq \mu_o < 0.3$:
 $T_{L1} = 6$
 $D/G_{o1} = 0.2 + \mu_o/3$
 if($G_{\max}/G_o < 0.4$) then fr = 0 else
 if($G_{\min}/G_o > (G/G_o)_{gr}$) then fr = 1 else
 if($G_{\max}/G_o > (G/G_o)_{gr}$ and $(G_{\max}/G_o - G_{\min}/G_o) < 0.1$) then fr = 1 else
 $T_{L2} = 8$
 $D/G_{o2} = 1.2G_{\min}/G_o$ then fr = $(G/G_o - D/G_{o2}) / (\mu_o I/G_o)$
 If $\mu_o \geq 0.3$:
 $T_{L3} = 10$
 $D/G_{o3} = 0.3$
 if($G_{\max}/G_o < 0.4$) then fr = 0 else
 if($G_{\min}/G_o > (G/G_o)_{gr}$) then fr = 1 else
 if($G_{\max}/G_o > (G/G_o)_{gr}$ and $(G_{\max}/G_o - G_{\min}/G_o) < 0.1$) then fr = 1 else
 $T_{L4} = 8$
 $D/G_{o4} = 1.2G_{\min}/G_o$ then fr = $(G/G_o - D/G_{o4}) / (\mu_o I/G_o)$

The Linke turbidity factors as well as the parameterizations of the diffuse radiation have been numbered for reference purposes when these will be adjusted in section 6.3.

The above algorithm is the basic form of the adjusted algorithm, in which the values for T_L as well as the parameterizations for the diffuse and direct radiation have been kept the same as in the Bergman algorithm. Whether these are realistic and will be kept in the eventual adjusted method is investigated in the next section by comparing them to radiation measurements. Further it will be checked whether $G_{\max}/G_o < 0.4$ is a good representation of completely cloudy periods and the differences in global radiation within a 10 minute interval will also be studied, to check whether $G_{\max}/G_o - G_{\min}/G_o < 0.1$ is in general true for cloudless periods.

6.2 Parameterizations and measurements

In the algorithm, the global irradiance for cloudless conditions (also called the limiting value, or $(G/G_o)_{gr}$) is estimated by the sum of estimates for the diffuse and direct irradiance under cloudless skies. If this limiting value is chosen as the lower limit of the global irradiance for cloudless periods, it will always be exceeded by the measured global irradiance when a period is indeed cloudless. If the measured global irradiance exceeds the limiting value within a 10 minute interval, at least G_{\max}/G_o will exceed $(G/G_o)_{gr}$, meaning that there was some sunshine during this interval. When also G_{\min}/G_o exceeds the limiting value, the whole period was cloudless and is thus determined as sunny.

Solar radiation measurements can now be used to obtain estimates of the lower limits of the diffuse and direct irradiance under cloudless conditions and these can be compared to the parameterizations that are used in the algorithm. For this study, 10 minute mean values of the different radiation components (I, G, D), as derived from radiation measurements between March 2005 and February 2006, are used. First cloudless days are selected. This is done by visual inspection of the direct irradiance during the day, which is a smooth curve with no large variations within 10 minute intervals (see for example Figure 5.9). Further also Total Sky Imager images are used to check if a day was indeed cloudless, resulting in 17 cloudless days, throughout the year.

After selecting cloudless days, the measured direct and diffuse irradiance can be plotted as a function of μ_o , which is done in Figure 6.1a and 6.1b respectively. Together with the measurements (in black), the parameterizations as used in the algorithm are shown (in red). Figure 6.1a shows that especially for $\mu_o > 0.3$ the current parameterization is not a realistic estimate of the direct irradiance for cloudless periods. For $\mu_o \geq 0.3$, T_L is chosen as 10 in the Bergman algorithm, which is much too high, given that normally T_L lies between 2 in winter and 6 in summer (Velds, 1992). The mean value of T_L for cloudless periods is indeed found to be 3.3 (averaged T_L on the selected cloudless days), so the green line ($T_L = 3.5$) in Figure 6.1a is representative of the mean direct irradiance under cloudless skies. An estimation of the lower limit of the direct irradiance under cloudless conditions is given by the blue line in Figure 6.1a ($T_L = 5.5$), but also $T_L = 5$ or $T_L = 6$ give reasonable estimates of this lower limit. This lower limit seems to be valid for all solar elevation angles, so possibly it is not necessary to treat the periods for which $\mu_o < 0.3$ different than those for which $\mu_o \geq 0.3$.

Figure 6.1b shows that the parameterization that is used in the algorithm for D/G_o (given by the red line) overestimates the diffuse irradiance for most μ_o . An estimate of the lower limit of the diffuse irradiance for cloudless periods is given by the blue line in Figure 6.1b.

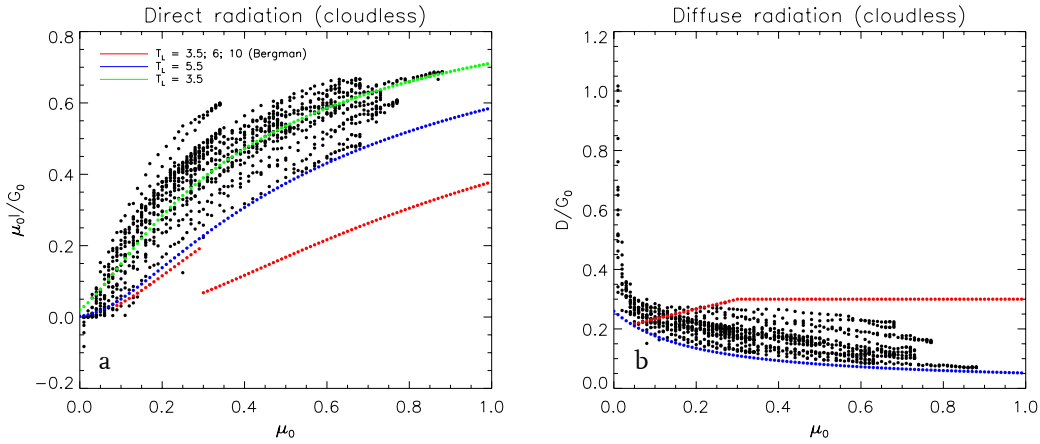


Figure 6.1: (a) Measurements of the normalised direct irradiance ($\mu_o I / G_o$) on a selection of 17 cloudless days as a function of μ_o (black). Also shown is the parameterization of Kasten: $\mu_o I / G_o = \exp(-T_L / (0.9 + 9.4\mu_o))$, with different values for T_L : $T_L = 3.5$; 6; 10 (red, values as used in the Bergman algorithm), $T_L = 5.5$ (blue) and $T_L = 3.5$ (green). (b) Measurements of the normalised diffuse irradiance (D / G_o) as a function of μ_o on cloudless days (black), the relation for D / G_o as used in algorithm ($D / G_o = 0.2 + \mu_o / 3$ for $\mu_o < 0.3$ and $D / G_o = 0.3$ for $\mu_o \geq 0.3$) (red) and $D / G_o = 0.01 + 1 / (20\mu_o + 4)$ (blue).

What can be concluded from Figure 6.1 is that the parameterizations that are used in the Bergman algorithm do not give an accurate estimation of the lower limit of the direct and diffuse irradiance under cloudless skies. Therefore, in the adjusted algorithm, these parameterizations will be replaced by the ones that are given in blue in Figure 6.1. To estimate the direct irradiance for cloudless periods, the parameterization of Kasten is used, with $T_L = 5.5$:

$$\mu_o I / G_o = \exp\{-T_L / (0.9 + 9.4\mu_o)\} \quad (6.1)$$

An estimation of the diffuse irradiance during cloudless periods is given by Equation (6.2):

$$D / G_o = 0.01 + 1 / (20\mu_o + 4) \quad (6.2)$$

Implementing these parameterizations makes the algorithm more realistic and understandable, since now $(G / G_o)_{gr} (= \mu_o I / G_o + D / G_o)$ will only be exceeded by the measured G / G_o when the period is indeed cloudless.

For the part of the algorithm that deals with partly cloudy situations, the fraction of sunshine is determined by the ratio of the actual direct irradiance ($G / G_o - D / G_o$) and the estimated direct irradiance for cloudless periods ($\mu_o I / G_o$). The actual direct irradiance is estimated by subtracting an estimated value for the diffuse irradiance for broken cloud situations from the measured global irradiance. For this part of the algorithm it is thus necessary to find a realistic estimation of the direct irradiance for cloudless periods. Figure 6.1 showed that the parameterization of Kasten with $T_L = 3.5$ is suitable for this (Equation (6.1) with $T_L = 3.5$). In the Bergman algorithm $T_L = 8$ was chosen for this part of the algorithm. This value for T_L is again too high, giving an underestimation of the direct irradiance under clear skies and thereby overestimating the

sunshine duration. Lowering T_L is thus believed to decrease the sunshine duration during broken clouds, and thereby to decrease the difference between SD_{Bergman} and SD_{Direct} . This concretizes suggestion 3. from section 5.5, which now obtains a form that can be used in the algorithm.

The diffuse irradiance for partly sunny situations is estimated by $1.2 G_{\text{min}}/G_o$. Like for cloudless days, now days on which broken clouds dominated were selected to be able to study the diffuse irradiance on these days, both as a function of G_{min} and of μ_o (Figure 6.2). Twenty days were selected for this study. $D/G_o = 1.2 G_{\text{min}}/G_o$ is a satisfactory parameterization for all μ_o , however, another possible parameterization is $D/G_o = 0.3$, since D/G_o was found to be approximately independent of μ_o . The scatter in the measurements is rather large, especially for the latter parameterization, but nevertheless both parameterizations will be tested in the adjusted algorithm.

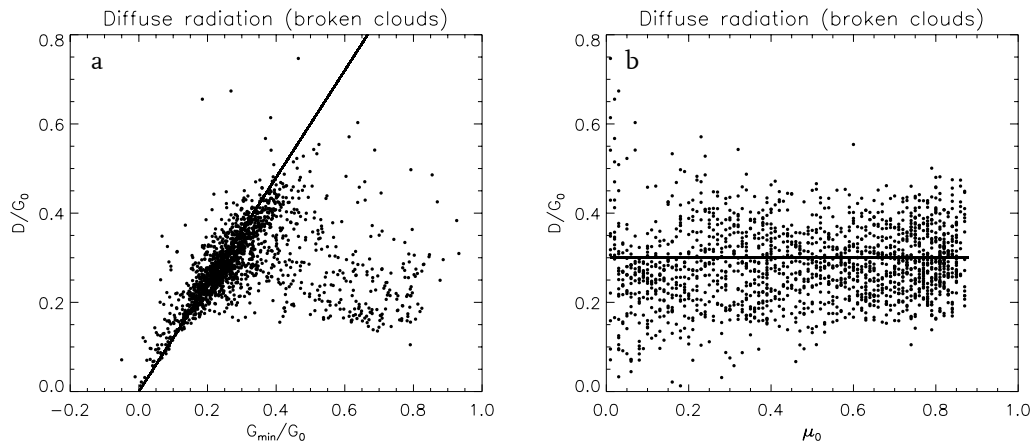


Figure 6.2: (a) Measurements of the diffuse irradiance (D/G_o) on a selection of 20 days with broken clouds as a function of (a) G_{min}/G_o and (b) μ_o . Also shown is a parameterization for D/G_o (solid lines): (a) $D/G_o = 1.2 G_{\text{min}}/G_o$ (as used in the Bergman algorithm) and (b) $D/G_o = 0.3$.

In the Bergman method, periods are determined as completely sunny when $G_{\text{min}}/G_o > (G/G_o)_{\text{gr}}$, or when $G_{\text{max}}/G_o > (G/G_o)_{\text{gr}}$ and $(G_{\text{max}}/G_o - G_{\text{min}}/G_o) < 0.1$. In Figure 6.3, measurements of $G_{\text{max}}/G_o - G_{\text{min}}/G_o$ for cloudless days are shown as a function of μ_o , together with the line $G_{\text{max}}/G_o - G_{\text{min}}/G_o = 0.1$. Figure 6.3 shows that for $\mu_o > 0.2$ $G_{\text{max}}/G_o - G_{\text{min}}/G_o < 0.1$ is valid on cloudless days, as is used in the Bergman algorithm. For $\mu_o < 0.2$ the difference between G_{max} and G_{min} is often larger than 0.1, so for small μ_o (for example $\mu_o < 0.3$) it might be desirable to increase this limit to 0.15 and thus still label periods as sunny when $G_{\text{max}}/G_o > (G/G_o)_{\text{gr}}$ and $(G_{\text{max}}/G_o - G_{\text{min}}/G_o) < 0.15$.

In the Bergman method, the fraction of sunshine duration is zero when $G_{\text{max}}/G_o < 0.4$, in a 10 minute interval. According to the WMO, the fraction of sunshine duration is zero when the DNSI does not exceed 120 Wm^{-2} , for 10 minute intervals this means that I_{max} should not exceed 120 Wm^{-2} . Figure 6.4 shows measurements of the maximum DNSI for every 10 minute interval (I_{max}) against the maximum normalised global irradiance per 10 minute interval (G_{max}/G_o). Also shown in Figure 6.4 are the lines $I_{\text{max}} = 120 \text{ Wm}^{-2}$ and $G_{\text{max}}/G_o = 0.4$. Figure 6.4 shows that for some periods $I_{\text{max}} > 120 \text{ Wm}^{-2}$, indicating a fraction of sunshine duration larger than zero, while $G_{\text{max}}/G_o < 0.4$, indicating a fraction of sunshine duration equal to zero. This means that in some cases the fraction of sunshine duration in an interval is erroneously given the value zero. This occurs in about 0.6 % of the cases. Decreasing the limit from 0.4 to 0.3 decreases the periods that are erroneously determined as cloudy to only 0.1 % of the cases. $G_{\text{max}}/G_o < 0.4$ is thus thought to be a good representation of completely cloudy periods (fraction of sunshine duration =

o), but in the adjusted algorithm also $G_{\max}/G_o < 0.3$ will be tested as the criterion for completely cloudy periods.

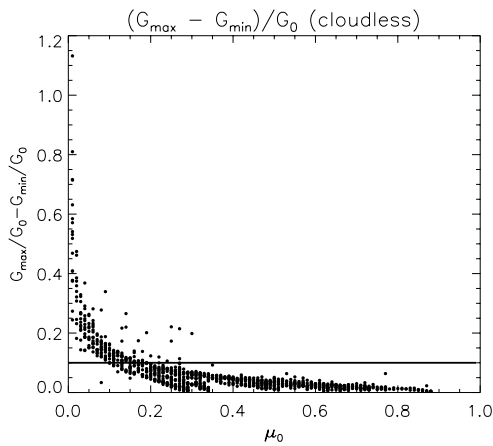


Figure 6.3: Measurements of $G_{\max}/G_o - G_{\min}/G_o$ on cloudless days as a function of μ_o and the line $G_{\max}/G_o - G_{\min}/G_o = 0.1$.

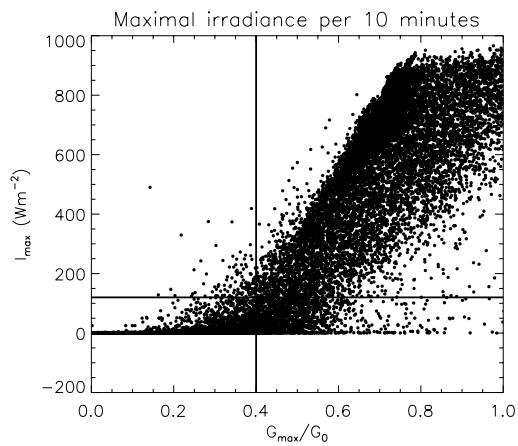


Figure 6.4: Measurements of the DNSI (maximum per 10 minute interval, in Wm^{-2}) against the normalised global irradiance (maximum G/G_o per 10 minute interval) (dots) and the lines $I_{\max} = 120 Wm^{-2}$ and $G_{\max}/G_o = 0.4$.

6.3 Sensitivity analysis

In the previous part, parameterizations that are used in the algorithm have been compared to radiation measurements. Not all parameterizations agreed with the measurements, and in these cases new parameterizations were suggested. In this part these parameterizations will be implemented in the algorithm and the sunshine duration will be determined with this adjusted algorithm. The reference, against which the adjusted algorithms will be compared, will be the Bergman algorithm, but the adjustments to be tested will not be implemented in the Bergman algorithm, but in the adjusted form of the algorithm as given in section 6.1 (called the basic form). The values of T_L and the parameterizations of D/G_o have been numbered in this algorithm, which will be used here to describe the adjustments made. Twelve adjusted algorithms (as described in Table 6.1) and their results will be compared.

For each adjusted algorithm and for the Bergman algorithm, the averaged difference per day between $SD_{\text{Algorithm}}$ and SD_{Direct} is given in Table 6.1, as well as the total sunshine duration for $\mu_o < 0.3$ and for $\mu_o \geq 0.3$. $SD_{\text{Algorithm}}$ refers to the sunshine duration that is determined by the pyranometric method, using a specific algorithm. The division in two μ_o -intervals is made to be able to study the effect of an adjustment for the lower and higher solar elevation angles separately, to find the best algorithm per interval and then combine these, as was suggested in section 5.5 (suggestion 4.). For $\mu_o < 0.3$, $\mu_o \geq 0.3$ and all μ_o together, scatterplots can be made of the daily $SD_{\text{Algorithm}}$ against the daily SD_{Direct} and a line can be fitted through the data-points. The slope and offset of these fits, as well as the spread of the data around the fit, are a measure of the agreement between the pyranometric and pyr heliometric method and are therefore also given in Table 6.1.

In all adjustments $D/G_{o1} = D/G_{o3} = 0.01 + 1/(20\mu_o + 4)$ (Equation 6.2), unless stated otherwise. In adjustment 1 to 4, $T_{L1} = T_{L3} = 5.5$ and $T_{L2} = T_{L4} = 3.5$.

Table 6.1: Sunshine duration for $\mu_o < 0.3$ and $\mu_o \geq 0.3$ (h/year) for the Bergman method (= reference) and different adjusted algorithms (adjustment 1 to 12 and the Linear algorithm). Also given is the averaged difference in sunshine duration with the pyrheliometric method (in h/d, $SD_{Direct} = 1429$ h/year). Further the daily $SD_{Algorithm}$ can be plotted against the daily SD_{Direct} and a fit can be plotted through the data. The slope and offset of this fit, as well as the spread (h) of the data around the fit are also given for the reference and each adjustment, for $\mu_o < 0.3$, $\mu_o \geq 0.3$ and all μ_o together. The last column gives the performance of the adjustment compared to the reference, where a + stands for improvement and a - for no improvement.

Adjustment	Averaged $SD_{Algorithm} - SD_{Direct}$ (h/d)	$SD_{\mu_o < 0.3}$ (h/y)	$SD_{\mu_o \geq 0.3}$ (h/y)	Spread (h) ($\mu_o < 0.3$ - $\mu_o \geq 0.3$ - all μ_o)	Slope ($\mu_o < 0.3$ - $\mu_o \geq 0.3$ - all μ_o)	Offset ($\mu_o < 0.3$ - $\mu_o \geq 0.3$ - all μ_o)	Per for ma nce
Pyrheliometric method		393	1036				
Reference: Bergman algorithm	0.59 ± 0.04	484	1135	0.39 0.61 0.74	1.00 0.97 0.97	0.28 0.41 0.70	
1: $T_{L1} = T_{L3} = 5.5, T_{L2} = T_{L4} = 3.5, D/G_{o2} = D/G_{o4} = 1.2 G_{min}/G_o$	-0.07 ± 0.05	493	915	0.42 0.69 0.85	1.00 0.86 0.89	0.31 0.08 0.40	- - -
2: $T_{L1} = T_{L3} = 5.5, T_{L2} = T_{L4} = 3.5, D/G_{o2} = D/G_{o4} = 0.3$	0.23 ± 0.04	482	1023	0.41 0.53 0.71	0.99 0.91 0.92	0.28 0.25 0.57	- + +
3: $T_{L1} = T_{L3} = 5.5, T_{L2} = T_{L4} = 3.5, G_{max}/G_o < 0.3$	0.53 ± 0.06	565	1037	0.66 0.57 0.94	0.95 0.91 0.90	0.60 0.30 0.96	-- - -
4: $T_{L1} = T_{L3} = 5.5, T_{L2} = T_{L4} = 3.5, G_{max}/G_o - G_{min}/G_o < 0.15$ ($\mu_o < 0.3$)	0.24 ± 0.04	484	1023	0.41 0.53 0.71	0.99 0.91 0.92	0.29 0.25 0.58	- + +
5: $T_{L1} = T_{L3} = 5, T_{L2} = T_{L4} = 3.5$	0.11 ± 0.04	468	996	0.38 0.50 0.67	0.99 0.90 0.92	0.24 0.20 0.46	+ + +
6: $T_{L1} = T_{L3} = 6, T_{L2} = T_{L4} = 3.5$	0.35 ± 0.05	492	1050	0.42 0.58 0.76	1.00 0.92 0.93	0.31 0.31 0.67	- - -
7: $T_{L1} = T_{L3} = 5.5, T_{L2} = T_{L4} = 3$	0.15 ± 0.04	478	1000	0.41 0.55 0.73	0.99 0.90 0.92	0.27 0.21 0.51	- - -
8: $T_{L1} = T_{L3} = 5.5, T_{L2} = T_{L4} = 4$	0.32 ± 0.04	486	1047	0.41 0.51 0.70	1.00 0.92 0.93	0.29 0.29 0.62	- + +
9: $T_{L1} = 5, T_{L2} = 3, T_{L3} = 5, T_{L4} = 4$	0.17 ± 0.04	462	1023	0.38 0.48 0.65	0.99 0.91 0.93	0.23 0.24 0.49	+ ++ ++
10: $T_{L1} = 5, T_{L2} = 3, T_{L3} = 5, T_{L4} = 4, D/G_{o1} = D/G_{o3} = 1/(20\mu_o + 4)$	0.21 ± 0.04	468	1028	0.39 0.50 0.67	0.99 0.91 0.93	0.25 0.26 0.52	+ + +
11: $T_{L1} = 5, T_{L2} = 3, T_{L3} = 5, T_{L4} = 4, D/G_{o1} = D/G_{o3} = 0.02 + 1/(20\mu_o + 4)$	0.14 ± 0.04	457	1018	0.37 0.47 0.64	0.98 0.91 0.93	0.22 0.24 0.47	+ ++ ++
12: $T_{L1} = 4, T_{L2} = 2.5, T_{L3} = 5, T_{L4} = 4, D/G_{o1} = 0.02 + 1/(20\mu_o + 4)$ (Improved algorithm)	0.02 ± 0.04	414	1022	0.31 0.48 0.61	0.96 0.91 0.92	0.12 0.24 0.36	++ ++ ++
Linear algorithm	0.03 ± 0.03	392	1045	0.31 0.39 0.51	0.95 0.98 0.96	0.06 0.09 0.20	++ ++ ++

The first adjustment to be discussed is the basic form, with $D/G_{o2} = D/G_{o4} = 1.2 G_{min}/G_o$. The averaged difference in sunshine duration is smaller for adjustment 1 than for the Bergman

method, which is an improvement. Beside the difference in sunshine duration, also the fit through the data and the spread of the data matter however. A smaller spread is associated with a better performance of the algorithm, as is a slope close to one and an offset close to zero. For adjustment 1, the spread is larger and the slope of the fit smaller than for the reference, so, as a whole, adjustment 1 is not an improvement of the Bergman method.

For adjustment 2, $D/G_{o2} = D/G_{o4} = 0.3$, which results in an improvement compared to adjustment 1 and the spread and total sunshine duration are improved compared to the reference as well. Therefore $D/G_{o2} = D/G_{o4} = 0.3$ is found to be an improvement and will be maintained in all other adjustments.

For the third adjustment $G_{max}/G_o < 0.3$ will be used instead of $G_{max}/G_o < 0.4$ as the criterion to select completely cloudy periods. This does not result in any improvement compared to adjustment 2 or the reference, so $G_{max}/G_o < 0.4$ will be kept as the criterion for completely cloudy periods in the algorithm.

Adjustment 4 checks whether periods with $G_{max}/G_o - G_{min}/G_o < 0.15$ should be labelled completely sunny for $\mu_o < 0.3$, since Figure 6.3 showed that $G_{max}/G_o - G_{min}/G_o < 0.1$ is only valid for cloudless periods for $\mu_o > 0.2$. However, adjustment 4 is no improvement compared to adjustment 2 or the reference, so $G_{max}/G_o - G_{min}/G_o < 0.1$ is kept as criterion to label periods cloudless when $G_{min}/G_o < (G/G_o)_{gr} < G_{max}/G_o$.

Compared to $T_{L1} = T_{L3} = 5.5$ and $T_{L2} = T_{L4} = 3.5$, T_{L1} and T_{L3} are lowered in adjustment 5, and raised in adjustment 6, while T_{L2} and T_{L4} are lowered in adjustment 7 and raised in adjustment 8 (Table 6.1). The results from adjustment 5 to 8 show that lowering T_{L1} , T_{L2} and T_{L3} and raising T_{L4} improves the algorithm.

For adjustment 9, 10 and 11, $T_{L1} = T_{L3} = 5$, $T_{L2} = 3$ and $T_{L4} = 4$ is chosen. In adjustment 9, nothing else is changed, which results in an improvement compared to adjustment 2 and the reference, but the sunshine duration for $\mu_o < 0.3$ is still too much. Adjustment 10, in which D/G_{o1} and D/G_{o3} are lowered to $1/(20\mu_o + 4)$, is found to be no improvement, but adjustment 11, in which D/G_{o1} and D/G_{o3} are raised to $0.02 + 1/(20\mu_o + 4)$, shows an improvement for $\mu_o < 0.3$.

Even for adjustment 11, the sunshine duration for $\mu_o < 0.3$ as determined with the algorithm is still much higher than that determined with the pyrheometric method. Therefore T_{L1} and T_{L2} are lowered even more, to $T_{L1} = 4$ and $T_{L2} = 2.5$, in adjustment 12. T_{L3} and T_{L4} are kept at the values 5 and 4 respectively. Further, $D/G_{o1} = 0.02 + 1/(20\mu_o + 4)$, while D/G_{o3} is kept at $0.01 + 1/(20\mu_o + 4)$. For $\mu_o < 0.3$, adjustment 12 is indeed an improvement compared to the reference and the other adjustments. Adjustment 12 is the best adjusted algorithm that we obtained; it will be referred to as the Improved algorithm and the pyranometric method using this algorithm as the Improved method.

In summary, the following adjustments have been made to the Bergman algorithm to obtain the Improved algorithm:

- The μ_o intervals $0.05 \leq \mu_o \leq 0.087$ and $0.087 < \mu_o < 0.3$ have been combined;
- The part of the algorithm that treats partly cloudy periods is applied to all μ_o instead of only to $\mu_o \geq 0.3$;
- For $0.05 \leq \mu_o < 0.3$ T_L has been adjusted: from 6 to 4 for the main part of the algorithm, and from 8 to 2.5 for the part of the algorithm that treats broken clouds;
- For $\mu_o \geq 0.3$ T_L has been adjusted: from 10 to 5 for the main part of the algorithm, and from 8 to 4 for the part of the algorithm that treats broken clouds;
- The parameterization of D/G_o has been adjusted:

- from $D/G_o = 0.2 + \mu_o/3$ to $D/G_o = 0.02 + 1/(20\mu_o + 4)$ for $\mu_o < 0.3$ (main part algorithm);
- from $D/G_o = 0.3$ to $D/G_o = 0.01 + 1/(20\mu_o + 4)$ for $\mu_o \geq 0.3$ (main part algorithm);
- from $D/G_o = 1.2G_{\min}/G_o$ to $D/G_o = 0.3$ (part of the algorithm that treats broken clouds).

Figure 6.5 and 6.6 show the results from comparing the Improved method to the pyrheliometric method. Figure 6.5 and 6.6 show that the difference with the pyrheliometric method is smaller for the Improved method than for the Bergman method (Figures 5.2 and 5.3).

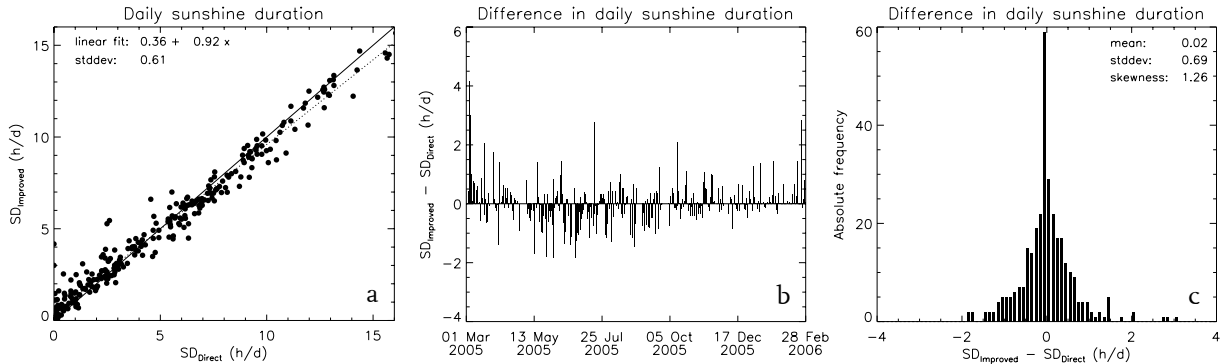


Figure 6.5: (a) Daily sunshine duration (h) according to the Improved method against the daily sunshine duration (h) according to the Direct method (points), a fit through the data (dotted line) and the 1:1 line (solid line). (b) Difference in daily sunshine duration (h) throughout the year ($SD_{Improved} - SD_{Direct}$). (c) Absolute frequency of $SD_{Improved} - SD_{Direct}$ (h/d).

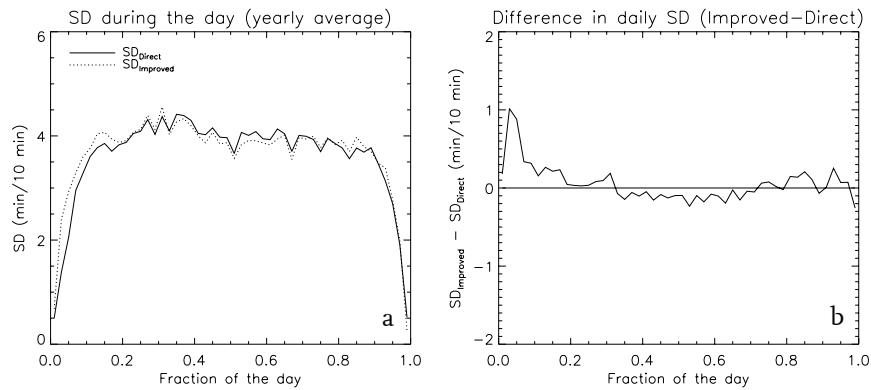


Figure 6.6: (a) Sunshine duration according to the Improved method (dotted line) and the Direct method (solid line) in minutes per 10 minute interval as a function of the day fraction (0=sunrise, 1=sunset), averaged over the period Mar 2005 – Feb 2006, (b) difference (Improved – Direct) in averaged sunshine duration in minutes per 10 minute interval as a function of the day fraction.

In Figure 6.5a the points gather more around the 1:1 line, Figure 6.5b shows that now positive as well as negative differences are observed and Figure 6.5c confirms that the differences in sunshine duration are more evenly spread around zero for the Improved method. Also the $SD_{Improved}$ during the day (Figure 6.6), averaged over the year, is in better agreement with the SD_{Direct} than was the $SD_{Bergman}$ (cf. Figure 5.3). The Improved algorithm is thus a significant improvement of the Bergman algorithm.

Table 6.1 shows that averaged over the year the daily difference between $SD_{Improved}$ and SD_{Direct} is approximately zero. However, this is partly caused by the fact that for $\mu_o < 0.3$ the Improved

method overestimates the sunshine duration compared to the Direct method, while it underestimates the sunshine duration for $\mu_0 \geq 0.3$. Figure 6.5a shows that overestimation of the sunshine duration occurs mostly on days with less than 5 hours of sunshine duration, while underestimation occurs on days with sunshine during more than 7 hours.

Since radiation measurements have been used to derive the parameterizations for the Improved algorithm, these are in better agreement with reality than the parameterizations used in the Bergman algorithm. However, the values that are used for the Linke turbidity factor for $\mu_0 < 0.3$ are quite low, leading to rather large values for the estimates of the direct irradiance and of its lower limit under cloudless skies. Instead of a realistic estimation of the direct irradiance for cloudless periods, an estimation of the upper limit is used, while a realistic estimation is used where a lower limit of the direct irradiance for cloudless periods is desired according to our idea of the algorithm. Besides, the estimation of the diffuse irradiance for cloudless periods is also rather high for $\mu_0 < 0.3$, closer to a realistic estimation of the diffuse irradiance under cloudless skies than a lower limit. So even though use has now been made of the measurements, eventually the best algorithm is obtained by tuning the parameterizations in the algorithm to fit the pyrheliometric sunshine duration. This also means that the best algorithm might be different when more years of data would be used, so that it is not for sure that the best possible algorithm has now been found.

6.4 A linear algorithm

So far, only adjustments of the Bergman algorithm have been studied. Another option would be to use an algorithm with a different form to determine the sunshine duration from global radiation measurements. This possibility is investigated by correlating pyrheliometric sunshine duration with global radiation. In Figure 6.7 SD_{Direct} is plotted against corresponding measurements of G/G_0 for (a) $\mu_0 < 0.3$ and (b) $\mu_0 \geq 0.3$. Figure 6.7 indicates that the relation between the sunshine duration and G is approximately linear. The correlation is such that below a certain lower limit of G/G_0 the sunshine duration is zero and above some upper limit it is 10

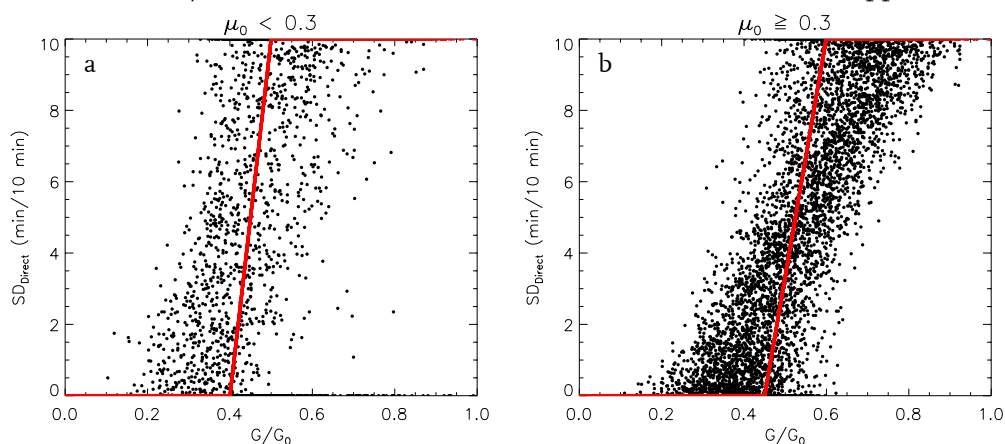


Figure 6.7: Measurements of SD_{Direct} (min/10 min interval) against G/G_0 (black) for (a) $\mu_0 < 0.3$ and (b) $\mu_0 \geq 0.3$. Also shown is a parameterization for the SD in terms of G/G_0 (red) (a) with lower limit 0.4, upper limit 0.5 and slope 100 and (b) with lower limit 0.45, upper limit 0.6 and slope 67.

minutes per 10 minute interval, while between the lower and upper limit the relation between the sunshine duration and G/G_0 is approximately linear. Figure 6.4 showed that $G/G_0 < 0.4$ is a

suitable condition for completely cloudy periods, and can thus serve as a lower limit. Likewise it can be shown that $G/G_o > 0.6$ is a suitable condition for completely sunny periods, thus serving as upper limit. For small μ_o the lower and upper limit are found to be smaller than for larger μ_o , indicating that a different parameterization for small μ_o is preferred over an algorithm without such a separation. The separation into different μ_o -intervals is again made at $\mu_o = 0.3$, since largest differences in upper and lower limit were found between the two intervals when the separation was chosen at this μ_o . A possible parameterization for sunshine duration in terms of G/G_o is also shown in Figure 6.7, in red.

The form of the linear algorithm is:

$$\begin{array}{lll}
 \mu_o < 0.3: & G/G_o < a & \rightarrow \text{fr} = 0 \\
 & a \leq G/G_o < b & \rightarrow \text{fr} = (G/G_o - a)/(b - a) \\
 & G/G_o \geq b & \rightarrow \text{fr} = 1 \\
 \\
 \mu_o \geq 0.3: & G/G_o < c & \rightarrow \text{fr} = 0 \\
 & c \leq G/G_o < d & \rightarrow \text{fr} = (G/G_o - c)/(d - c) \\
 & G/G_o \geq d & \rightarrow \text{fr} = 1
 \end{array}$$

With a and c the lower limits for respectively the interval $\mu_o < 0.3$ and $\mu_o \geq 0.3$, and b and d the corresponding upper limits. Further, the slopes of the linear relation between the sunshine duration and G/G_o that is valid between the lower and upper limit is determined by a , b , c and d and is $1/(b-a)$ for $\mu_o < 0.3$ and $1/(d-c)$ for $\mu_o \geq 0.3$.

The algorithm has been optimized by variation of the lower and upper limits. For each combination of upper and lower limit, the averaged difference in sunshine duration between this pyranometric method and the pyrheliometric method is determined, as well as the total sunshine duration for $\mu_o < 0.3$ and for $\mu_o \geq 0.3$. As before, the daily $SD_{\text{Algorithm}}$ can be plotted against the daily SD_{Direct} and a fit can be plotted through the data. For $\mu_o < 0.3$, the best results are found with a lower limit of 0.4 and an upper limit of 0.5 , while for $\mu_o \geq 0.3$ a lower limit of 0.45 and an upper limit of 0.6 give the best results. Variation of the μ_o at which separation into two intervals takes place does not provide further improvement. The best linear algorithm is thus:

$$\begin{array}{lll}
 \mu_o < 0.3: & G/G_o < 0.4 & \rightarrow \text{fr} = 0 \\
 & 0.4 \leq G/G_o < 0.5 & \rightarrow \text{fr} = (G/G_o - 0.4)/0.1 \\
 & G/G_o \geq 0.5 & \rightarrow \text{fr} = 1 \\
 \\
 \mu_o \geq 0.3: & G/G_o < 0.45 & \rightarrow \text{fr} = 0 \\
 & 0.45 \leq G/G_o < 0.6 & \rightarrow \text{fr} = (G/G_o - 0.45)/0.15 \\
 & G/G_o \geq 0.6 & \rightarrow \text{fr} = 1
 \end{array}$$

These are the parameterizations shown in Figure 6.7, which means that the performance of the algorithm is determined mainly by the upper and lower limits and that it is less important how well the slope of the parameterization fits the measurements. This is caused by the fact that for most 10 minute intervals the fraction of sunshine duration is either 0 or 1, for $\mu_o \geq 0.3$ this is the case for about 70% of the intervals, while for $\mu_o < 0.3$ this is even the case for 87% of the intervals. The measurements corresponding to either $SD = 0$ or $SD = 10$ minutes per 10 minute interval are therefore most important in determining the linear algorithm, explaining why a linear

fit that seems to fit the measurements well, does not give the best results when used in the algorithm. Figure 6.8 shows the accompanying scatterplot of the daily SD_{Linear} against the daily SD_{Direct} for this algorithm, which will be referred to as the Linear algorithm. The pyranometric method using this algorithm will be called the Linear method. Figure 6.9 shows the sunshine duration during the day.

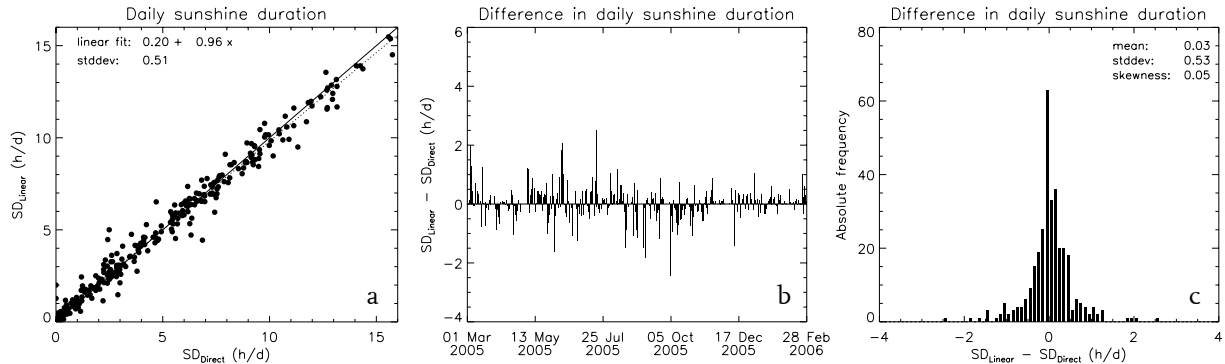


Figure 6.8: (a) Daily sunshine duration (h) according to the Linear method against the daily sunshine duration (h) according to the Direct method (points), a fit through the data (dotted line) and the 1:1 line (solid line). (b) Difference in daily sunshine duration (h) throughout the year ($SD_{Linear} - SD_{Direct}$). (c) Absolute frequency of $SD_{Linear} - SD_{Direct}$ (h/d).

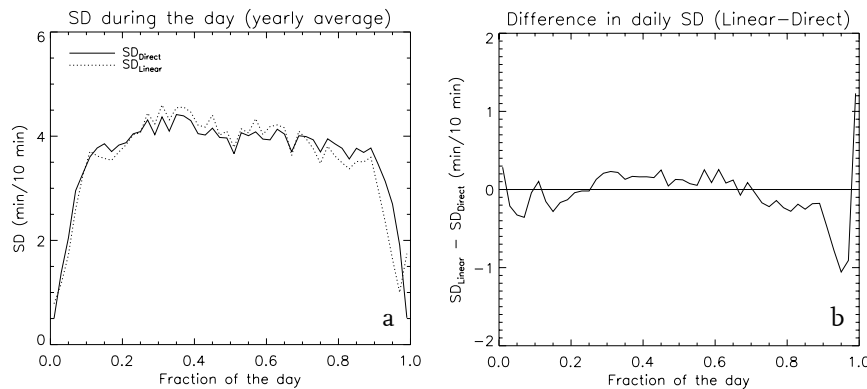


Figure 6.9: (a) Sunshine duration according to the Linear method (dotted line) and the Direct method (solid line) in minutes per 10 minute interval as a function of the day fraction (0=sunrise, 1=sunset), averaged over the period Mar 2005 – Feb 2006, (b) difference (Linear – Direct) in averaged sunshine duration in minutes per 10 minute interval as a function of the day fraction.

For the Linear method, the average difference in sunshine duration with the pyrheliometric method, the sunshine duration for $\mu_o < 0.3$ and $\mu_o \geq 0.3$ and the spread, slope and offset of the fit in Figure 6.8a are given in the last row of Table 6.1. Comparison of the results from the Linear method to the Improved method shows that the Linear algorithm performs better. The yearly averaged difference in daily sunshine duration is small for both adjusted methods, but for the Improved method an overestimation of the sunshine duration for $\mu_o < 0.3$ is compensated by an underestimation of the sunshine duration for $\mu_o \geq 0.3$, while for the Linear algorithm this is not the case. Further, the offset is smaller for the Linear method, the slope closer to one and the spread of the data is much smaller. As mentioned, Figure 6.5a (Improved method) still shows an overestimation of the sunshine duration, compared to the pyrheliometric method, on days with only a few hours of sunshine duration and an underestimation of the sunshine duration on days with more sunshine duration, while this is not the case in Figure 6.8a (Linear method), where the

data gather more round the 1:1 line. Figure 6.8b and 6.8c show that the daily differences in sunshine duration between the Linear and pyr heliometric method are spread quite evenly around zero. Further it can be concluded from Figure 6.9 that the Linear method also gives improved values of the sunshine duration during the day, averaged over the year, compared to the Bergman method.

Finally, the sunshine duration during the different months and seasons as determined with the Direct, Bergman, Improved and Linear method is compared in Figure 6.10. This shows that indeed the Linear as well as the Improved method are improvements of the Bergman method. During most months, the agreement between the Linear method and the Direct method is equal or better than for the Improved method, except in April and October. The performance of the Improved method is better than that of the Linear method in autumn, but worse in summer and winter, as can be seen in Table 6.2 that shows the difference in sunshine duration per season between the different pyranometric methods and the pyr heliometric method.

Table 6.2: Differences in sunshine duration between the different pyranometric methods and the pyr heliometric method during the different seasons and during the year.

	Spring	Summer	Autumn	Winter	Year
$SD_{\text{Bergman}} - SD_{\text{Direct}}$ (h)	61	50	44	34	191
$SD_{\text{Improved}} - SD_{\text{Direct}}$ (h)	7	-14	1	13	7
$SD_{\text{Linear}} - SD_{\text{Direct}}$ (h)	8	7	-12	5	8

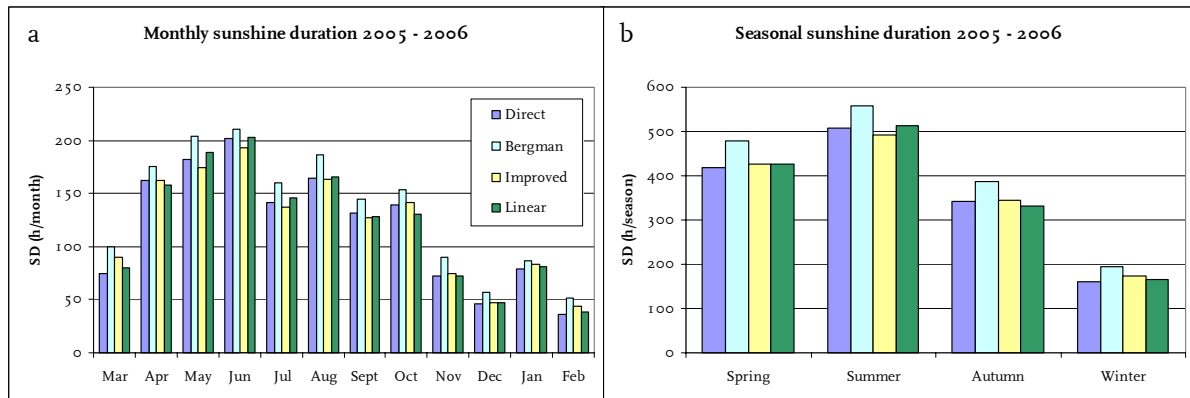


Figure 6.10: (a) Monthly and (b) seasonal totals of sunshine duration (h) according to the Direct, Bergman, Improved and Linear method.

In conclusion we can state that the Linear algorithm is the best algorithm that we found. Despite being derived rather simplistic, with coarse parameterizations, the performance of the Linear method is better than that of the Slob, Bergman or Schipper method.

7. Sunshine duration from a sunshine duration sensor

7.1 The CSD

So far, the pyrheliometric method and different versions of the pyranometric method have been used to determine the sunshine duration. Another way of determining the sunshine duration is by means of a different instrument that is specifically designed to measure the sunshine duration. The Kipp & Zonen Sunshine Duration sensor (CSD, where the C is added for reasons of nomenclature), as shown in Figure 7.1, is such an instrument that offers a relatively simple way of measuring the sunshine duration (Kipp & Zonen, 2003).

The principle of the CSD is that it uses three detectors D_1 , D_2 and D_3 that each cover part of the sky. D_1 detects all the solar radiation, direct and diffuse, while D_2 and D_3 only cover $1/3$ of the sky; the part that is covered by D_2 is not seen by D_3 . First it is determined whether D_2 or D_3 is receiving direct irradiance (maximum signal). Then the detector with the smallest signal is chosen, and this output is thought to represent approximately $1/3$ of the diffuse irradiance. The value of D_1 is then reduced by the estimated value of the



Figure 7.1: The CSD3 at the Cabauw BSRN site.

diffuse irradiance to obtain an estimate of the direct irradiance I : $I = D_1 - C \cdot (\text{smallest of } D_2 \text{ and } D_3)$, where D_1 , D_2 , D_3 are the signals of detectors D_1 , D_2 , D_3 and C is a geometry factor.

The value of the direct irradiance is then compared to the WMO threshold of 120 Wm^{-2} , and a period is labelled sunny when the direct irradiance exceeds 120 Wm^{-2} . The CSD can also supply a derived value of the direct irradiance itself, although this signal is not a substitute for pyrheliometer measurements since it does not have the same level of accuracy.

The instrument has been designed in such a way that it can be used anywhere on Earth in a fixed position. Further the three detectors have exactly the same spectral and angular characteristics, making the process of recalibration easy. Other advantages of the CSD are that it has low power consumption and an integrated heater. In climates where dew, frost or ice can exist heating is of particular importance, since it improves the reliability of the measurements in these climates. Furthermore, there are no moving parts involved, such as a sun-tracker needed for pyrheliometer measurements. Therefore this instrument is believed to offer a relatively cheap and accurate alternative for the pyrheliometric sunshine duration.

The best location for the installation of the CSD is a place where the sun is visible the entire day without any obstructions at the horizon, but at least the direct irradiance should not be blocked. The instrument should be installed parallel to the north-south plane, pointing towards the nearest pole. Further, the angle between the instrument axis and a horizontal plane should be equal to the latitude of the installation location. The maintenance of the CSD is limited, only regular cleaning of the transparent window is recommended.

December 2005 a CSD3, the third version of the CSD instrument as developed by Kipp & Zonen, was installed at Cabauw (Figure 7.1). The accuracy of sunshine hours as determined by the CSD3 is said to be more than 90% in monthly totals of sunshine duration. Further, the spectral range is 400 to 1100 nm, the response time less than 1 ms and the accuracy of the direct irradiance more than 90% for clear skies. Measurements of the CSD3, at a sampling rate of 1 second, are available from December 8th 2005 on, meaning that it is possible to compare the sunshine duration from the CSD to the sunshine duration from the pyrheliometric and pyranometric methods for the winter of 2005-2006.

7.2 Direct irradiance

Figure 7.2 shows minute mean values of the direct normal solar irradiance as estimated from the CSD measurements against minute mean values as measured with the pyrheliometer, for the winter season. It is clear from Figure 7.2 that there is a good correlation between the two direct irradiance values, but also that the CSD in general overestimates the direct irradiance. Only for very high values of the pyrheliometric DNSI the CSD underestimates the DNSI, but for the purpose of sunshine duration determination the larger DNSI are not important. The values of the DNSI around 120 Wm^{-2} are important for the sunshine duration analysis, and here the DNSI as

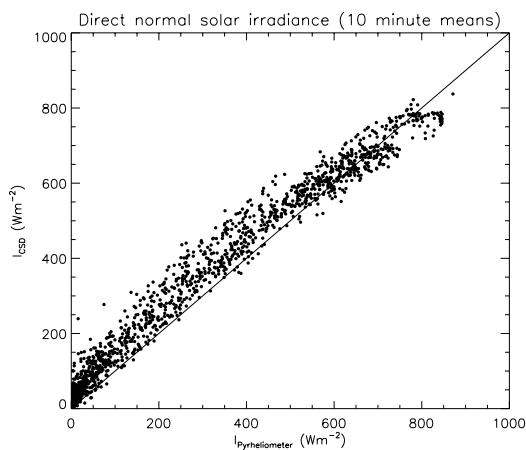


Figure 7.2: Ten minute means of the DNSI (Wm^{-2}) derived from measurements of the CSD versus pyrheliometric measurements for the winter 2005-2006.

estimated by the CSD is found to be about 60 Wm^{-2} too high. So the CSD overestimates the sunshine duration. Introducing an offset correction factor of 60 Wm^{-2} and subtracting this from the DNSI estimated from the CSD measurements will reduce this overestimation. In the following section the sunshine duration as determined from the original CSD measurements will be compared to that determined from CSD measurements after subtracting the correction factor. Furthermore, these results will be compared to the sunshine duration as determined with the pyranometric method using either the Bergman or the Linear algorithm.

7.3 Sunshine duration determined by the CSD

Since the CSD instrument was installed at Cabauw at the beginning of December, it is possible to determine the sunshine duration with the CSD during the winter season. Data from December 8th 2005 – February 28th 2006 is used for this analysis. Besides the days already specified in section 4.1, also February 23rd 2006 (daynumber 54) is omitted from the analysis. This is done because the difference in sunshine duration between the pyrheliometric method and the CSD is much larger on this day than on all other days, therefore playing a dominant role when a fit is plotted through the data, and distorting the results. So even though no clear cause could be found for this large deviation, this day was omitted from the sunshine duration determination. Figure

7.3 shows the daily SD_{CSD} against the daily SD_{Direct} and the differences in daily sunshine duration, plotted as a function of time and in a histogram. It is clear from Figure 7.3a that the performance of the CSD is close to that of the Direct method, since the spread in the data is small and the points gather near the 1:1 line. Figures 7.3b and 7.3c show that mainly positive differences occur, meaning that on average the CSD overestimates the sunshine duration compared to the pyrheliometric method. The overestimation of the sunshine duration by the CSD is 0.18 hours per day, averaged over the winter (Table 7.1). Also given in Table 7.1 are the total sunshine duration during winter, the cumulative difference and the averaged difference per day for the CSD and the Bergman and Linear method. Figure 7.4 shows the scatterplots for the Bergman and Linear methods.

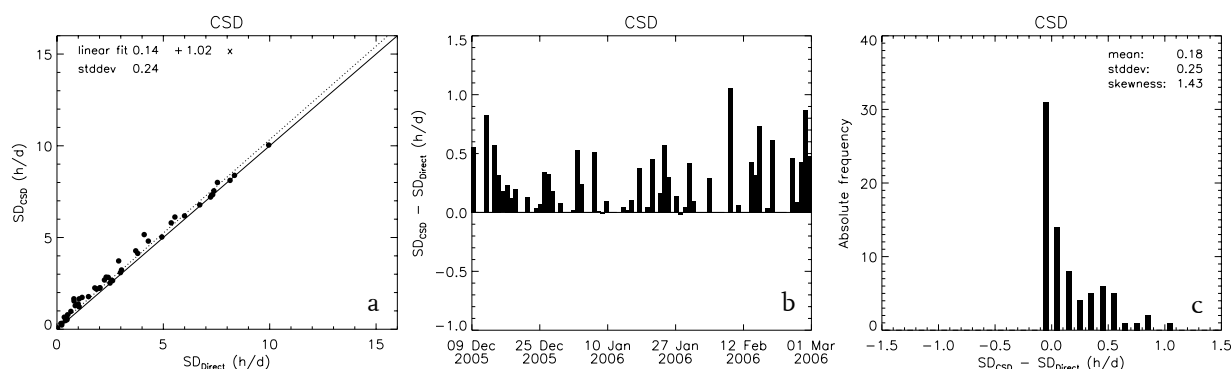


Figure 7.3: (a) Daily sunshine duration (h) according to the CSD against the daily sunshine duration (h) according to the Direct method (points), a fit through the data (dotted line) and the 1:1 line (solid line). (b) Difference in daily sunshine duration (h) throughout the winter ($SD_{CSD} - SD_{Direct}$). (c) Absolute frequency of $SD_{CSD} - SD_{Direct}$ (h/d).

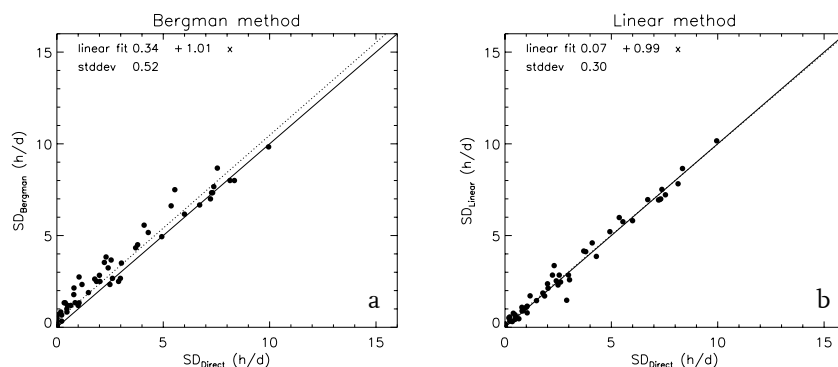


Figure 7.4: Daily sunshine duration (h) according to (a) the Bergman method and (b) the Linear method, against the daily sunshine duration according to the Direct method for December 2005 – February 2006 (points) also a fit through the data (dotted line) and the 1:1 line (solid line) are shown.

Table 7.1: Winter totals of sunshine duration as determined with the Bergman and Linear method and with the CSD and CSD-60 method (h) ($SD_{Direct} = 150$ h/winter). Also given are the cumulative difference (h/y) and the averaged difference per day (h/d) between each method and the pyrheliometric method.

Method	Bergman	Linear	CSD	CSD-60
Sunshine duration during winter (h/winter)	179	155	165	151
Cumulative difference ($SD_{Method} - SD_{Direct}$) (h/winter)	29	5	15	1
Averaged difference per day ($SD_{Method} - SD_{Direct}$) (h/d)	0.37 ±	0.06 ±	0.18 ±	0.00 ±
	0.06	0.03	0.03	0.01

Comparison of Figure 7.3a, 7.4a and 7.4b shows that the spread in the data is smallest for the CSD, but for the Linear method the points are spread more evenly around the 1:1 line. Table 7.1 confirms that the averaged difference per day is smallest for the Linear method, so that on average the Linear method gives the best results. The results of the CSD are much better than of the Bergman method though, as expected, since the CSD is designed to measure sunshine duration.

So far, DNSI estimates of the CSD have been used to determine the sunshine duration. Now a correction factor is taken into account and the DNSI estimates are lowered by 60 Wm^{-2} before the sunshine duration is determined (the value of 60 Wm^{-2} as offset correction factor is determined empirically, by determining the sunshine duration from the CSD measurements with different values for the correction factor and comparing the results to the pyr heliometric sunshine duration). We use a correction factor because Figure 7.2 showed that the DNSI according to the CSD is higher than that measured by the pyr heliometer, especially around 120 Wm^{-2} ; the value of importance for sunshine duration determination. This method of sunshine duration determination will be referred to as the CSD-60 method. The results from the CSD-60 method are given in Table 7.1 and Figure 7.5.

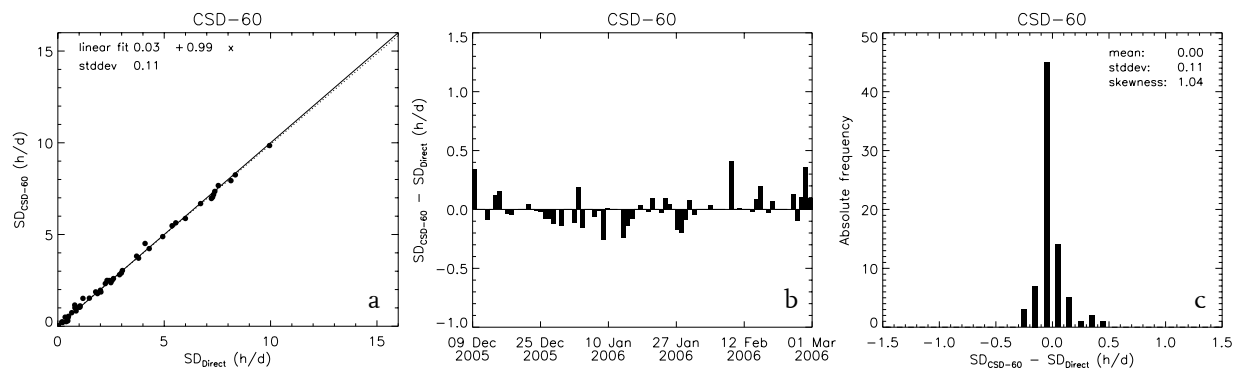


Figure 7.5: (a) Daily sunshine duration (h) according to the CSD-60 method against the daily sunshine duration (h) according to the Direct method (points), a fit through the data (dotted line) and the 1:1 line (solid line). (b) Difference in daily sunshine duration (h) throughout the winter ($SD_{CSD-60} - SD_{Direct}$). (c) Absolute frequency of $SD_{CSD-60} - SD_{Direct}$ (h/d).

Comparison of Figures 7.3, 7.4 and 7.5 shows that the sunshine duration as determined with the CSD-60 method is closest to the sunshine duration as determined with the pyr heliometric method. This means that the CSD can be almost as accurate as the pyr heliometer in determining the sunshine duration, when a correction factor is taken into account for the CSD measurements.

The accuracy of sunshine hours as determined by the CSD3 is claimed to be more than 90% in monthly totals of sunshine duration. With the measurements currently available it is possible to check this for the winter of 2005 – 2006. From the values given in Table 7.1 it can be derived that for the winter season as a total, $(SD_{CSD} - SD_{Direct})/SD_{Direct} * 100\% = 11\%$, meaning that the accuracy of sunshine hours as determined by the CSD3 is 89% for the winter season (without use of correction factor). The accuracy per month is investigated in Table 7.2, which shows that in January the accuracy is indeed more than 90%, but that this criterion is not met in December and February. It can thus be said that the accuracy of the CSD is about 90% for monthly totals of sunshine duration, but that it deviates from month to month. It must be mentioned however that only a short dataset has been used here, and that inspection of more data is required to be able to come to a definitive conclusion.

Table 7.2: Monthly sunshine duration (h) according to the CSD and to the Direct method for the winter of 2005 – 2006. Also given is the difference in sunshine duration between the two methods relative to SD_{Direct} (%) and the accuracy of the CSD with respect to the pyrliometric method (%).

	December 2005	January 2006	February 2006
SD_{Direct} (h/month)	38	79	33
SD_{CSD} (h/month)	42	83	39
$(SD_{\text{CSD}} - SD_{\text{Direct}}) / SD_{\text{Direct}}$ (%)	11	5	18
Accuracy of SD_{CSD} (%)	89	95	82
Accuracy of $SD_{\text{CSD-60}}$ (%)	100	99	96

For comparison, also the accuracy of the CSD-60 method is given in Table 7.2. For this method the accuracy of monthly totals of sunshine duration is larger than 90% during all months. This shows that the accuracy of CSD measurements of sunshine duration can be significantly improved by using an on-site calibration by means of a pyrliometer to find a correction factor that can be taken into account to correct for the general overestimation of the DNSI by the CSD.

8. Summary and conclusions

In this report we study and compare three methods for the determination of sunshine duration from solar radiation measurements. The first method, the pyr heliometric method, is based on measurements of the direct solar irradiance, made with a pyr heliometer mounted on a sun tracker. This method relies directly on the WMO definition of sunshine duration: “sunshine duration during a given period is defined as the sum of that sub-period for which the direct solar irradiance exceeds 120 Wm^{-2} .” The second method is based on 10-minute mean measurements of global solar irradiance with a pyranometer and (parameterized) estimates of the direct and diffuse irradiance. The measured difference between the minimum and maximum value of the global irradiance during the 10-minute interval is used to determine whether or not there is a temporary eclipse of the sun by clouds. The method is referred to as pyranometric method and was originally designed by Slob and Monna (1991). According to these authors, the uncertainty is about 0.6 h for daily sums of sunshine duration. Two variations of the original algorithm are also considered in this report. For historical reasons, Bergman (1993) adjusted the original algorithm to find more agreement with sunshine duration values derived from the traditional Campbell-Stokes sunshine recorder. This adjusted algorithm is used by KNMI to estimate the sunshine duration for a network of 32 meteorological stations in the Netherlands. Schipper (2004) adjusted the original algorithm to find more agreement with the pyr heliometric sunshine duration. The third method for the determination of sunshine duration discussed in this report is based on indirect measurements of the direct irradiance made with an instrument specifically designed for the detection of sunny periods. Since it does not contain moving parts, such as the sun tracker for the pyr heliometer, this instrument is believed to offer a relatively cheap and accurate alternative for the pyr heliometric sunshine duration.

The main objective of this report is to evaluate the pyranometric method as used by KNMI in the national network. Furthermore, it is attempted to improve the pyranometric method. For this purpose, we use measurements of direct, diffuse, and global irradiance made at the Baseline Surface Radiation Network (BSRN) site in Cabauw, the Netherlands. The site is equipped with state of the art radiation instruments which allow for a detailed comparison of the three methods introduced above. Starting point of all comparisons presented here is the application of the WMO definition of sunshine duration to a 1-year data set (March 2005 – February 2006) of pyr heliometric measurements of direct solar irradiance acquired with a sampling frequency of 1 Hz. These measurements give “sunshine seconds” which form the basis for the “true” sunshine duration, in hours per day, month, season, or year.

According to the pyr heliometric method the cumulative “true” sunshine duration for the period mentioned is 1429 h. This deviates from the yearly averaged sunshine duration over the Netherlands (1534 h for the period 1971-2000) because 41 days were omitted from the analysis, due to problems with the data acquisition system, power loss or sun-tracking problems on these days. The three pyranometric methods give 1357 h (original algorithm), 1620 h (operational algorithm), and 1546 h (Schipper algorithm). The differences between the pyranometric and pyr heliometric values are thus considerable: -72 h, +191 h, and +117 h, respectively, or, expressed as a percentage of the pyr heliometric sunshine duration, -5%, +13% and 8%. On a daily average basis, the differences amount to $-0.22 \pm 0.05 \text{ h/d}$, $0.59 \pm 0.04 \text{ h/d}$, and $0.36 \pm 0.06 \text{ h/d}$, for the original, operational and Schipper algorithm respectively. It thus appears that the original pyranometric method, designed by Slob and Monna (1991), gives yearly

cumulative and daily average values for the sunshine duration which are closest to “true” (WMO) sunshine duration. The algorithm that is operationally used by KNMI significantly overestimates the “true” sunshine duration. This is not surprising because this algorithm has been tuned to the sunshine duration obtained by the Campbell-Stokes sunshine recorder. The Campbell-Stokes measurements are rather uncertain and tend to overestimate the sunshine duration, especially during broken-cloud conditions. The Schipper algorithm appears to be not an improvement of the original algorithm, in terms of yearly cumulative sunshine duration, but also in terms of daily totals, since the variations in the differences per day are found to be largest for the Schipper algorithm.

Given the large yearly difference in sunshine duration between the operational algorithm and the pyr heliometric method, improvement of the pyranometric method is desired. We investigated the possibility of improving the operational algorithm by means of a sensitivity analysis, in which the parameterizations as used in the algorithm are varied. Solar radiation measurements are used as basis for the new parameterizations, after which the parameterized estimates of clear-sky direct and diffuse irradiance are tuned to the pyr heliometric sunshine duration. It appears that with adjustments of the atmospheric turbidity and parameterized diffuse irradiance closer agreement with the “true” sunshine duration can be obtained: with this improved algorithm the yearly cumulative sunshine duration becomes 1436 h. The difference between the pyranometric method using this improved algorithm and the pyr heliometric method reduces to only +7 h (0.5% of the pyr heliometric sunshine duration) for the whole period, and 0.02 ± 0.04 h/d on daily average basis. At this point the improved algorithm thus performs much better than the operational algorithm. On daily basis, the improved algorithm is, however, still overestimating the sunshine duration for small solar elevation angles and underestimation is found for the larger solar elevation angles.

Although the improved algorithm performs rather well, we also investigated the possibility of a completely different algorithm, in which the global radiation is directly related to sunshine duration. This algorithm consists of a lower limit for the global radiation below which periods are completely cloudy and an upper limit for the global radiation above which periods are completely sunny. For the global radiation between the lower and upper limit, the sunshine duration is linearly related to the global radiation, which is why we will call this the linear algorithm. The algorithm distinguishes between two different solar elevation angle intervals ($\mu_0 < 0.3$ and $\mu_0 \geq 0.3$), with different values for the lower and upper limits, since for smaller solar elevation angles better results are obtained if lower values are chosen for the lower and upper limits. The algorithm is optimized with respect to the pyr heliometric sunshine duration by variation of the upper and lower limits, resulting in a cumulative sunshine duration of 1437 h. This gives a cumulative difference of +8 h (0.6% of the pyr heliometric sunshine duration) between the pyranometric method using the linear algorithm and the pyr heliometric method, and a difference of 0.03 ± 0.03 h/d on daily average basis. This means that, on yearly basis, the improved and linear algorithm perform equally well and are both improvements compared to the original and the operational algorithm. However, the linear algorithm does not overestimate the sunshine duration for small solar elevation angles or overestimate the sunshine duration for larger solar elevation angles, meaning that the diurnal variations in sunshine duration are better represented by the linear algorithm, so that on daily basis it performs better than the improved algorithm. Compared to the improved algorithm, the linear algorithm is more transparent. The linear algorithm can therefore be adjusted more systematically, making tuning to the “true” sunshine duration easier.

The third method for the determination of sunshine duration that we investigated is based on measurements of the Kipp & Zonen CSD, an instrument specifically designed to measure sunshine duration. This instrument was installed at Cabauw December 2005, only allowing for comparisons for the winter season. According to the different methods, the cumulative sunshine duration during this season is 150 h (pyrheliometric method). The other methods give 179 h (pyranometric method using the operational algorithm), 155 h (pyranometric method using the linear algorithm) and 165 h (CSD). These values correspond to differences with respect to the pyrheliometric sunshine duration of +29 h, +5 h, and +15 h, respectively. On a daily average basis the differences amount to 0.37 ± 0.06 h/d, 0.06 ± 0.03 h/d, and 0.18 ± 0.03 h/d, respectively. The agreement between sunshine duration determined with the CSD measurements and the pyrheliometric sunshine duration is larger than between the pyrheliometric method and the pyranometric method using the operational algorithm. Especially the variation in daily differences is found to be smallest for the CSD. However, on average, the CSD still overestimates the sunshine duration. This can be solved by applying a calibration correction (offset of -60 Wm^{-2}) to the CSD direct irradiance: the cumulative sunshine duration then becomes 151 h, reducing the cumulative difference with the pyrheliometric method to only +1 h and the daily averaged difference to only 0.00 ± 0.01 h/d. This indicates that the sunshine duration as determined by means of CSD measurements can be almost as accurate and precise as the sunshine duration determined with the pyrheliometric method, when the CSD measurements are calibrated against pyrheliometric measurements of the direct irradiance. The cumulative sunshine duration determined with the CSD is very close to that obtained with the pyrheliometer measurements, but on individual days small deviations still exist.

The current analysis of sunshine duration determination is based on a one-year dataset. A recommendation for future research is therefore to apply the linear algorithm to a multi-year dataset, to study whether the linear algorithm is still the best algorithm to use in the pyranometric method to estimate the sunshine duration from global radiation measurements. Furthermore, it would also be interesting to test this algorithm using measurements made in a different latitude, to investigate its performance under different solar elevation conditions. With respect to the improved algorithm additional evaluation is probably less urgent because the algorithm is basically the same as the original algorithm.

The present study makes it possible to obtain more accurate sunshine duration estimates on the basis of global radiation measurements. By using either the improved or the linear algorithm instead of the operational (KNMI) algorithm, the overestimation of the sunshine duration by the pyranometric, compared to the pyrheliometric method, can be reduced from 13% to only 0.6%, on yearly basis. We recommend to process and archive at KNMI two sunshine duration products:

1. a product that is generated only for the purpose of continuation of the Campbell-Stokes record of sunshine duration. For this product, the currently operational algorithm (Bergman, 1993) should be used.
2. a product that gives best agreement with the WMO definition of sunshine duration. We suggest that only this product is used for external purposes, such as seasonal or annual overviews of the sunshine duration and tourism. For this product the improved algorithm, as proposed in this study, should be used. Alternatively, the linear algorithm can be used, giving even better estimates of the sunshine duration. However, before implementing this algorithm, it is desirable to evaluate the algorithm with additional measurements made at e.g. the Cabauw BSRN site.

Acknowledgements

I want to thank Wouter Knap for his enthusiastic supervision of this study at the KNMI. Further I would like to thank Han van Dop for being my supervisor at the University of Utrecht, thereby enabling me to complete my meteorology education with this final project. Besides, at KNMI, I want to thank Cor van Oort for providing the solar radiation measurements, Alexander Los for answering various questions and Ed Worrell for his pictures of the instruments at the Cabauw site. Furthermore, I would like to thank Bruce Forgan (Bureau of Meteorology, Australia) for the e-mail correspondence about sunshine duration determination.

Symbols and acronyms

γ_o	solar elevation angle
θ_o	solar zenith angle
μ_o	$= \sin(\gamma_o) = \cos(\theta_o)$, represents the position of the sun with respect to the Earth
BSRN	Baseline Surface Radiation Network
d	day
D	diffuse solar irradiance (Wm^{-2})
DNSI	direct normal solar irradiance (Wm^{-2})
fr	fraction of sunshine in a 10 minute interval, multiplying by 10 gives the sunshine duration in minutes per 10 minute interval
G	global solar irradiance on a horizontal surface (Wm^{-2})
G_o	solar irradiance on a horizontal surface, outside the atmosphere (Wm^{-2})
$(G/G_o)_{gr}$	limiting value, estimation of the normalised global radiation for cloudless conditions
h	hour
I	direct normal solar irradiance (Wm^{-2})
I_o	solar irradiance at sun-Earth distance (Wm^{-2})
KNMI	Koninklijk Nederlands Meteorologisch Instituut (Royal Netherlands Meteorological Institute)
SD	sunshine duration
$SD_{\text{Algorithm}}$	sunshine duration as determined with a specified algorithm
SD_{Bergman}	sunshine duration as determined with the Bergman method
SD_{CSD}	sunshine duration as determined with the CSD sunshine duration sensor
$SD_{\text{CSD-60}}$	sunshine duration as determined with the CSD after subtracting 60 Wm^{-2} from the direct normal solar irradiance as estimated by the CSD
SD_{Direct}	sunshine duration as determined with the Direct method
SD_{Improved}	sunshine duration as determined with the Improved method
SD_{Linear}	sunshine duration as determined with the Linear method
SD_{Method}	sunshine duration as determined with a specified method
$SD_{\text{Pyranometric}}$	sunshine duration as determined with a pyranometric method (Bergman, Improved, Linear, Schipper or Slob method)
$SD_{\text{Pyrheliometric}}$	sunshine duration as determined with the pyrheliometric method (Direct method)
SD_{Schipper}	sunshine duration as determined with the Schipper method
SD_{Slob}	sunshine duration as determined with the Slob method
T_L	Linke turbidity factor, measure of the attenuation of solar radiation through extinction by aerosols and water vapour in the atmosphere
WMO	World Meteorological Organization
y	year

References

- Al-Sadah, F.H. and F.M. Ragab. Study of global daily solar radiation and its relation to sunshine duration in Bahrain. *Solar Energy*, **47** (2): 115–119 (1991).
- Ångström, A. Solar and Terrestrial Radiation. *Quarterly journal of the Royal Meteorological Society*, **50**: 121–125 (1924).
- Bergman, U. Het programma voor berekening van zonneshijnduur uit globale straling. Technische Rapporten; TR – 158. KNMI, De Bilt (1993).
- Cloudnet Database: Images of the Total Sky Imager. (<http://www.yesinc.com/products/data/tsi440/index.html>; http://www.knmi.nl/samenw/cloudnet/realtime/rt_img_tsi.html) (2006).
- Coulson, K.L. Solar and Terrestrial Radiation. Academic Press, New York [etc.], 215–234 (1975).
- Dyson, P. and B.W. Forgan. Investigation of the Uncertainty of Sunshine Duration in the Solar and Terrestrial Radiation Network. Instrument test report 674. Commonwealth Bureau of Meteorology (2003).
- El-Metwally, M. Sunshine and global solar radiation estimation at different sites in Egypt. *Journal of Atmospheric and Solar-Terrestrial Physics*, **67**: 1331–1342 (2005).
- Forgan, B.W. and P. Dyson. Uncertainty in Daily Sunshine Duration from BSRN Minute Statistics. ARIC – Bureau of Meteorology, BSRN July 2004 presentation (2004).
- Frantzen, A.J. and W.R. Raaff. De relatie tussen de globale straling en de relatieve zonneshijnduur in Nederland. Scientific report, WR – 82 – 5. KNMI, De Bilt (1982).
- Glickman, T.S. (Managing Editor). Glossary of Meteorology, Second Edition. American Meteorological Society, Boston, Massachusetts, USA (2000).
- Gopinathan, K.K. A general formula for computing the coefficients of the correlation connecting global solar radiation to sunshine duration. *Solar Energy*, **41** (6): 499–502 (1988).
- Hussain, M. et al. Techniques to obtain improved predictions of global radiation from sunshine duration. *Renewable Energy*, **18**: 263–275 (1999).
- Iqbal, M. An introduction to solar radiation. Academic Press, Toronto [etc.] (1983).
- Kasten, F. A simple parameterization of the pyrheliometric formula for determining the Linke turbidity factor. *Meteorol. Rdsch.* **33**: 124–127 (1980).

- Kipp & Zonen. CSD1 Sunshine Duration Meter, Instruction Manual. (<http://www.kippzonen.com>) (2003).
- Klimaatatlas van Nederland. KNMI, De Bilt (2002).
- Linke, F. Transmissions-Koeffizient und Trübungsfaktor. *Beiträge zur Physik der freien Atmosphäre*, **10**: 91-103 (1922).
- Liou, K.N. An Introduction to Atmospheric Radiation. Academic Press, Inc., Amsterdam [etc.] (2002).
- Long, C.N. and E.G. Dutton. BSRN Global Network recommended QC tests, V2.0. (<http://bsrn.ethz.ch>).
- Michalsky, J.J. The Astronomical Almanac's Algorithm For Approximate Solar Position (1950 - 2050). *Solar Energy*, **40** (3): 227-235 (1988).
- Ohmura, A. et al. Baseline Surface Radiation Network (BSRN/WCRP): New Precision Radiometry for Climate Research. *Bulletin of the American Meteorological Society*, **79** (10): 2115-2136 (1998).
- Schipper, J. Vergelijking van diverse methodes voor de berekening van zonneschijnduur uit globale straling. Technisch Rapport; TR - 258. KNMI, De Bilt (2004).
- Slob, W.H. and W.A.A. Monna. Bepaling van directe en diffuse straling en van zonneschijnduur uit 10-minuutwaarden van de globale straling. Technische Rapporten; TR - 136. KNMI, De Bilt (1991).
- Velds, C.A. Zonnestraling in Nederland. Thieme/KNMI, Baarn/De Bilt (1992).
- WMO CIMO Guide No. 8 (1996). WMO Guide to Meteorological Instruments and Methods of Observation. Sixth Edition (Chapter 7 and 8) (1996).

